Project acronym and title:
SECURe – Subsurface Evaluation of Carbon capture and storage and Unconventional risks

REPORT ON THE EFFECTIVENESS OF GAS AND MICROBIAL SENSORS AND HOW THEY WILL LINK IN WITH CURRENT BASELINE MONITORING STRATEGIES IN WP3

Authors and affiliation:

Jurgen P.T. Foeken, Cjestmir de Boer

TNO, The Netherlands

Tanya Goldberg

GFZ, Germany

Tina B. Bech

GEUS, Denmark

Megan J. Barnett, Simon P. Gregory

BGS, UK

Wolfram Kloppmann

BRGM, France

Email of lead author:
jurgen.foeken@tno.nl

Deliverable 4.6
Revision:1

Project funded by the European Commission within the Horizon 2020 Programme	
Dissemination Level	
PU	*Public*
~~***CO***~~	~~*Confidential, only for members of the consortium (incl. the Commission Services)*~~
~~***CL***~~	~~*Classified, as referred to in Commission decision 2001/844/EC*~~

Deliverable number:	D4.6
Deliverable name:	Report on the effectiveness of gas and microbial sensors and how they will link in with current baseline monitoring strategies in WP3
Work package:	WP4. Advanced monitoring and sensor technologies
Lead WP/deliverable beneficiary:	Matteo Icardi

Status of deliverable		
	By	**Date**
Submitted (Author(s))	Jurgen Foeken	18.03.21
Verified (WP leader)	Matteo Icardi	31.03.21
Approved (EB member)	Jonathan Pearce	31.03.21
Approved (Coordinator)	E HOUGH	31.03.21

Author(s)		
Name	**Organisation**	**E-mail**
Jurgen Foeken	TNO	jurgen.foeken@tno.nl
Cjestmir de Boer	TNO	cjestmir.deboer@tno.nl
Tanya Goldberg	GFZ	goldberg@gfz-potsdam.de
Tina Bech	GEUS	tib@geus.dk
Megan Barnett	BGS	megan@bgs.ac.uk
Simon Gregory	BGS	simongr@bgs.ac.uk
Wolfram Kloppmann	BRGM	w.kloppmann@brgm.fr

Public introduction

Subsurface Evaluation of CCS and Unconventional Risks (SECURe) is gathering unbiased, impartial scientific evidence for risk mitigation and monitoring for environmental protection to underpin subsurface geoenergy development. The main outputs of SECURe comprise recommendations for best practice for unconventional hydrocarbon production and geological CO_2 storage. The project is funded from June 2018–May 2021.

The project is developing monitoring and mitigation strategies for the full geoenergy project lifecycle; by assessing plausible hazards and monitoring associated environmental risks. This is achieved through a program of experimental research and advanced technology development that includes demonstration at commercial and research facilities to formulate best practice. We will meet stakeholder needs; from the design of monitoring and mitigation strategies relevant to operators and regulators, to developing communication strategies to provide a greater level of understanding of the potential impacts.

The SECURe partnership comprises major research and commercial organisations from countries that host shale gas and CCS industries at different stages of operation (from permitted to closed). We are forming a durable international partnership with non-European groups; providing international access to study sites, creating links between projects and increasing our collective capability through exchange of scientific staff.

Executive report summary

This report summarizes the research conducted within subtasks 4.3.1 and 4.3.2, a joint collaboration between TNO (The Netherlands, GFZ (Germany), GEUS (Denmark), BGS (UK) and BRGM (France). The effectiveness of novel isotope based methodologies and microbial analyses to monitor gas seepages were studied. Methods aimed at in-situ detection of gas seepages used clumped isotopes to study the origin of methane and/or CO_2 gas by determining its (subsurface) gas formation temperature. The response of microbial communities to in-situ gas leaks was characterised to identify if microbial groups can be used for monitoring purposes. Specifically, the bacterial community is described by long read of the 16S rRNA gene and the relative abundance of two functional genes (*pmoA* and *mcrA*). To test if long-term, time averaged records of CO_2 gas seepages can be reconstructed, Carbon-14 dating was conducted on local vegetation (leaves and tree rings).

Key summary of main results and conclusions:

- Methane clumped isotopes and calculated gas formation temperatures provide indications of the origin of deep, thermogenic gas vs. shallow biogenic gas;
- Methane clumped isotope gas samples that are in thermodynamic equilibrium provide gas formation temperatures that are in line with source rock burial temperatures predicted from basin models;
- Integrating methane clumped isotope temperatures with basin modelling and burial curves may be used to determine the source of the gas seeping to the surface;
- For routine gas seepage monitoring purposes, bulk isotope analyses on gasses provide faster and (currently) cheaper alternatives compared to methane clumped isotopes;
- Carbon-14 dating on tree ring and leaves from vegetation in the vicinity of gas seepages may provide some indications of long-term CO_2 seeps;
- Field laboratories studies mean DNA sequence data could be available within a few hours of sample collection, which is important to investigate spurious readings;
- No clear separation in microbial communities exposed to biogenic and thermogenic gas were observed, although in current studies thermogenic gas samples had much wider diversity;
- Methane oxidising indicator microorganisms could be detected by DNA analysis, however those of thermogenic origin were detected in very low numbers;
- Amplification of targeted DNA in the microbial communities (qPCR) suggest high relative abundance of the *mcrA* and *pmoA* genes are linked to biogenic methane and low abundance to thermogenic methane, which may allow discrimination of the methane origin.

The novel monitoring tools can be used to detect and monitor gas leakages at different spatial and temporal ranges. Outstanding research challenges need to be addressed before the techniques can be used for routine monitoring. Methane clumped isotope analyses is currently analytically challenging making it less suited for routine gas leakage monitoring. Based on the research presented here, a workflow for in-situ monitoring would involve repeated gas sampling campaigns for bulk isotope analyses ($\delta^{13}C$ and δD) with occasional sampling for clumped isotope analyses when additional insights in the origin of the gas are required.

From the work conducted in Sleen and France, it was concluded that microbial communities have the potential to be used as a monitoring tool. For specific gene types (*pmoA* and *mcrA*) it was demonstrated that the relative abundance of these genes is correlated to the gas isotopic composition with a higher relative abundance of both genes in biogenic gas (compared to a thermogenic origin). The work presented in this report suggests that combining microbial techniques with established geochemical (isotope) methods allows for assessment of the source of leaking gas.

Contents

FIGURES

TABLES

1 Introduction

Detection of present and past subsurface gas seepage and leakage (either natural origin or anthropogenic) is key in order to apply mitigation measures to reduce emissions of methane (CH_4) and/or carbon dioxide (CO_2). In the present SECURe research, a combination of novel isotope based methodologies and microbial analyses was used to decipher the origin and long-term baseline monitoring of gas seepages. First, short-term methods for in-situ determination of the origin of methane and/or CO_2 gas focused on deciphering its (subsurface) formation temperature by utilising clumped isotopes. Second, a methodology to test if and how local vegetation absorbs carbon from a CO_2 leak source was studied and compared to long-term time-averaged reference baseline by utilising Carbon-14 dating. Third, the response of microbial communities to gas leaks was characterised to identify if specific microbial groups can be used for monitoring purposes. This latter research builds on work presented in SECURe deliverable D4.3 (2021).

Because methane and CO_2 are important greenhouse gases, their formation and migration through the subsurface is important to help determine their contribution to the global methane/CO_2 flux (e.g., Etiope, 2009). Established techniques use the isotopic composition of these gasses, in particular the $\delta^{13}C$ ($^{13}C/^{12}C$) and δD (D/H) ratios, as tracers for determining their origin and migration pathways. Previous studies have determined distinct isotopic ratios that are indicative for the gas formation and migration processes involved. For example, methane gas that is formed from cracking during deep-seated hydrocarbon expulsion (so called thermogenic gas) has a distinct different $\delta^{13}C$ and δD composition compared to methane gas that formed in response to microbial processes in the shallow subsurface (so called biogenic gas) (e.g., Hoefs, 2009; Schoell, 1980). Microbial methanogenesis produces distinctly different isotope fractionations with methane produced by CO_2 reduction resulting in lower $\delta^{13}C$ values whereas methane produced from methylated compounds or acetate fermentation results in lower δD values (e.g., Douglas et al., 2017 and references therein). However, post-generation processes may also affect the isotopic composition in methane making the distinction between thermogenic and biogenic sources at times challenging (e.g., Whiticar, 1999).

Hence the availability of additional isotopic tracers would benefit in deciphering gas origins. Clumped isotopes have been suggested as a versatile tool for determining the gas formation temperature. “Clumped isotopes” refer to the bonding of two rare (heavier) isotopes in a molecule (e.g., Eiler, 2007). For CO_2, the clumping involves the bonding between the two heavy isotopes ^{13}C and ^{18}O in CO_2 (e.g., Eiler, 2007). More recently clumping in methane has also been researched and it was shown that for different geological settings, formation temperatures for thermogenic, microbial and abiotic methane could be reconstructed provided that the isotopic system formed in equilibrium (e.g., Douglas et al., 2017; Stolper et al., 2015; Stolper et al., 2014b; Young et al., 2017).

Establishing long-term, time averaged baseline reference is useful for determining past gas seepages prior to routine gas monitoring. The application of tree-ring analysis has been postulated to serve as a monitoring tool for (past) CO_2 emissions (e.g., Cook et al., 2001; Donders et al., 2013). Through the measurement of the radioactive isotope composition in dendro-dated tree rings or tree leaves, a site-specific atmospheric CO_2 record can be reconstructed. This local record may then be used to detect offsets in CO_2 fluxes between the (long-term) atmospheric carbon composition versus the CO_2 record incorporated into the tree rings or leaves (e.g., Donders et al., 2013). Carbon-14 (^{14}C) dating is a versatile tool for detecting this as ^{14}C is radioactive with a half live of about 5.7ka. Hence CO_2 emitted from (deep) subsurface sources (e.g. through hydrocarbon seeps) do not contain ^{14}C, meaning that emission of this ‘dead’ carbon in the form of CO_2 locally alters the radioactive carbon isotopic composition of the atmosphere (Donders et al., 2013). Trees take up this ^{14}C-depleted CO_2 and incorporate it into their wood and leaves. Consequently, deviations of the14C concentration relative to the mean atmospheric composition could be used as a proxy in reconstructing the spatial extent of seepage sites as well as temporal variability (Donders et al., 2013).

The use of microbial monitoring for the detection of gas seeps is further explored in this report and builds on research conducted in SECURe deliverable D4.3 (2021). Oil and gas microbial prospecting techniques rely on detecting changes to soil microbial communities caused by gas seeping through microfractures (Wagner et al., 2002). Atmospheric compositions above active gas fields have been observed to have an increased methane component with a disproportionate amount of alkanes such as propane and butane compared to biogenic sources of methane, strongly suggesting origin is the gas field (Karion et al., 2013). This results in detectable changes to the microbial communities in the soil, particularly methane, ethane, propane and butane oxidisers, or the relationships between them. These have all been used as indicators of gases leaking from

hydrocarbon deposits (Rasheed et al., 2013). This work builds on the same principal of the development of different microbial communities in the presence of biogenic and thermogenic gas sources but applied here to groundwater samples rather than soil samples for the purpose of monitoring rather than as a prospecting tool.

In SECURe report D4.3 (2021), total bacterial community analysis based on short reads of the 16S rRNA gene was tested as a proxy for detection of gas seepages from collected groundwater samples. In the present report, the bacterial community is further described by long read of 16S rRNA gene and the relative abundance of the two functional genes (particulate methane monooxygenase (*pmoA)* and methyl co-enzyme M reductase (*mcrA*)) as described below.

Of the microorganisms known to respond to gas leaks, methanotrophs (organisms able to oxidise methane) are a subset of the methylotrophs that can oxidise single carbon molecules, such as methane and methanol (unless otherwise stated, the term methanotrophs is used to describe organisms capable of oxidising methane, while methylotrophs describe the broader group of organisms capable of oxidising single carbon molecules, including methane).

In SECURe report D4.3 (2021), total bacterial community analysis based on short reads of the 16S rRNA gene was tested as a proxy for detection of gas seepages from collected groundwater samples. In the present report, the bacterial community is further described by long read of 16S rRNA gene and the relative abundance of the two functional genes (*pmoA* and *mcrA*).

Of the microorganisms known to respond to gas leaks, methanotrophs (organisms able to oxidise methane) are a subset of the methylotrophs that can oxidise single carbon molecules, such as methane and methanol (unless otherwise stated, the term methanotrophs is used to describe organisms capable of oxidising methane, while methylotrophs describe the broader group of organisms capable of oxidising single carbon molecules, including methane). In aerobic methanotrophs, methane is oxidized via methanol, formaldehyde, and formate to carbon dioxide. The key enzyme, methane monooxygenase, initiates this process. Nearly all aerobic methanotrophs possess a particulate methane monooxygenase, while the distribution of sMMO is more limited. Therefore, *pmoA* genes encoding for the alpha-subunit of the particulate methane monooxygenase are considered as a marker for the detection of aerobic methanotrophs (Knittel and Boetius, 2009).

The *mcrA* gene, specifically the alpha subunit methyl co-enzyme M reductase (Luton et al., 2002) has evolved as the essential marker gene for studying the diversity methanogenic archaea, but is also carried out by related anaerobic methane oxidizing archaea (ANME). The presence of this gene indicates methanogenic archaea or ANME, and sequencing of this gene would allow for the separation of the two processes. Specific archaea carry out biological methane production from types of carbon source; CO_2, acetate and methylated compounds. Similarly, sequencing can shed light onto which carbon source is used. Commonly, the final enzymatic reaction of all three pathways leading to methane production is always carried out by methyl co-enzyme M reductase which means methanogens utilizing all three pathways can be detected in a single assay.

2 Field sites

In order to test a range of novel analytical monitoring techniques, gas, water, soil, tree stem sections and leaves have been collected from three field sites: natural gas seepages (Fontaine Ardente and Rochasson, the French Alps), a gas reservoir (Borzęcin, Poland) and a man-induced methane leakage site (Sleen, The Netherlands). A variety of techniques were tested to assess their readiness for leakage monitoring purposes. In the French Alps, methane and CO_2 gas samples were collected to reconstruct the origin and formation temperature of the gas. Reconstructing long-term CO_2 seepage at this site was tested using Carbon-14 (^{14}C) dating on tree rings and plant leaves. Microbial community responses to gas leaks were tested to identify whether specific microbial groups can be used for monitoring of gas seepages in groundwater. Similar methods were tested at Sleen, with the exception of ^{14}C dating. Detailed subsurface data is available from hydrocarbon exploration at the Sleen site, which allows detailed cross calibration between the novel (isotope) techniques versus established methods for determining the origin of natural gas. At the Polish Borzęcin site, natural gas was sampled at an independent site to test the application of isotope technologies for reconstructing the gas formation origin.

2.1 FONTAINE ARDENTE AND ROCHASSON (FRENCH ALPS)

The Fontaine Ardente (FA) and Rochasson (ROC) natural gas seepage sites are located southwest (FA) and east (ROC) of Grenoble (Figure 1 and Figure 2). At FA, the gas is thought to originate from Callovian (Middle Jurassic) mudstones and argillaceous limestones. The site is located along a small seepage close to the river bed of a small creek the Vernant (Figure 1). Gas seepage is thought to migrate upward along small faults but the geometry of these faults remains unclear (e.g., Gal et al., 2017). Recent isotope studies have shown that the source of the gas has a thermogenic signature (SECURe Report D3.4, 2021). The gas seepage site at ROC is located along the flank of a thalweg and is linked to a small landslide in clayey horizons. Unlike FA, the seep at ROC does not burn spontaneously and the rate of CH_4 seepage is considerably lower (Gal et al., 2017). Further geological descriptions of the FA and ROC are provided in SECURe deliverable D3.4 (2021).

2.2 SLEEN (THE NETHERLANDS)

During drilling of an exploration gas well into Triassic sandstones in the 1960s, unexpected well control issues were experienced and downhole gas pressure build up resulted in an underground blowout of the well. Within hours of the uncontrolled blowout, an approximately 350m wide crater had formed from which natural gas erupted for nearly 3 months until a newly drilled relief well allowed for chocking the gas leakage (e.g., Schout et al., 2018).

The Sleen gas field consists of a series of Triassic sand and claystone layers (the Main Bundsandstein Subgroup) located at ~1900m depth. Gas is capped in these layers by a more than 100-m-thick deposit of evaporites of the Röt Formation. Potential source rocks for the gas include Carboniferous (Westphalian) coal and black shale intervals from the Limburg Group and Carboniferous Limestone Group (at present day buried to 3600-5400m depth, NITG-TNO, 2000).

Following the blowout, the local drinking water company installed several groundwater wells for monitoring possible adverse effects on groundwater quality at and around the blowout site (Figure 3). At the location of the blowout, the water table varies seasonally between 1 and 2 m below ground surface. The direction of groundwater flow is toward the south and east. The shallow subsurface geology (down to ~150m depth), is dominated by a thick succession of Quaternary sands and gravels (Figure 4). From top to bottom, the succession consists of glacial, fine- to medium-grained sand (Peelo Formation), fluvial coarse sand and gravel deposits (Appelscha Formation) and marine fine sand and clay (Oosterhout Formation).

The groundwater wells at Sleen are composed of well screens at different depth in the same wellbore (Figure 4A). Each well is backfilled with impermeable clays both below and on top of the screened interval to ensure hydraulic isolation (Schout et al., 2018).

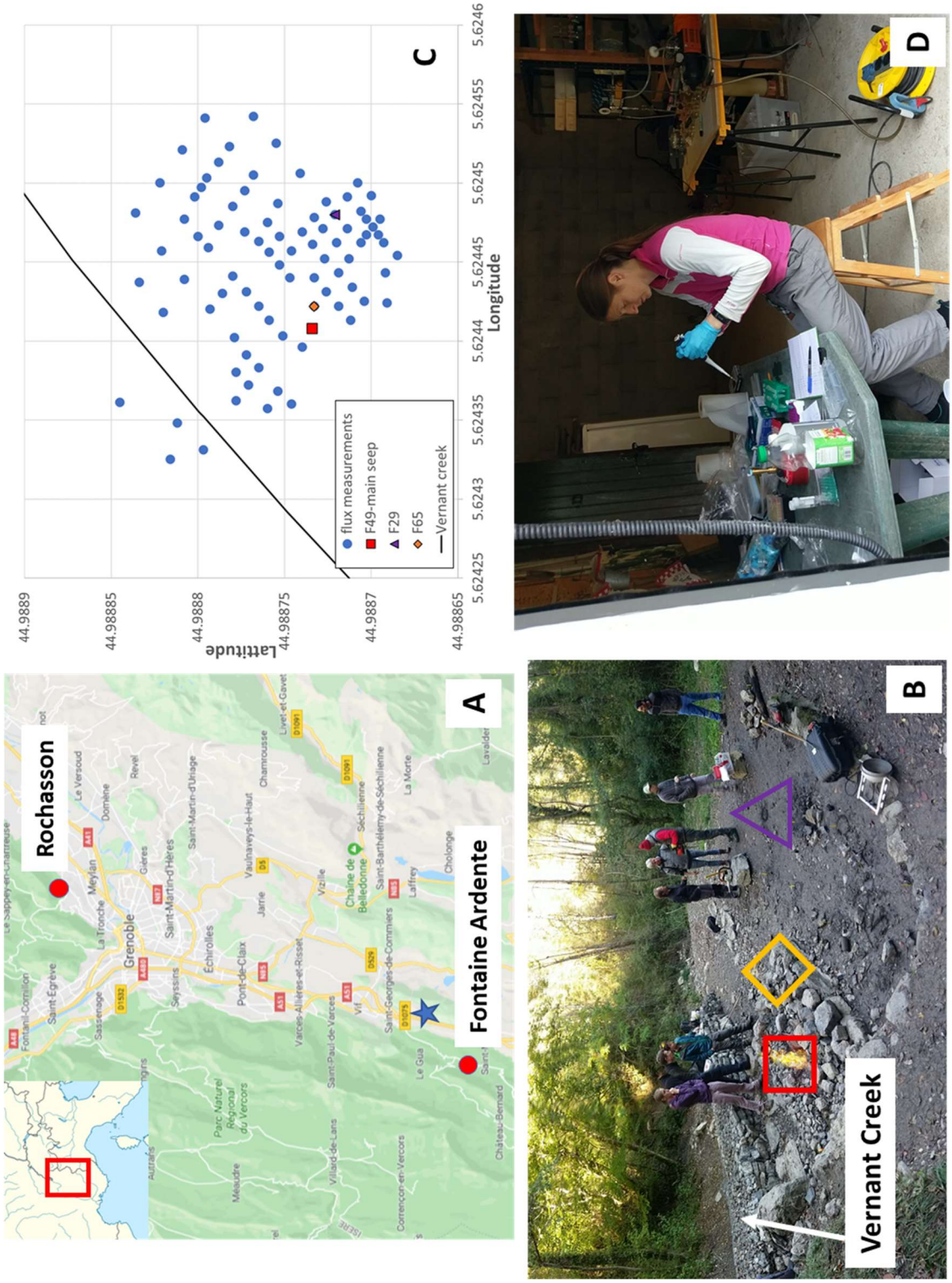

Figure 1: A. Location of the natural gas seepage sites in the French Alps (Fontaine Ardente and Rochasson) and the field laboratory for DNA sample preparation (blue star). B. Fontaine Ardente (FA) location. Red square=sample FA49 (main vent), orange diamond =sample FA65 (side vent) and purple triangle=sample FA29 (soil sample). C. Soil flux measurements (blue dots) with location of the collected gas samples (see SECURe Report D3.4, 2021 for results). D. Photo of the field laboratory for DNA sample preparation.

Owing to the blowout, the (shallow) subsurface stratigraphy is likely severely perturbed. A recent groundwater monitoring study showed that significant amounts of methane are still leaking through the subsurface into the groundwater system (Schout et al., 2018). Isotopic analyses of the groundwater and dissolved methane gasses showed that in the vicinity of the blowout site, elevated methane concentrations were found that had a thermogenic (deep gas reservoir) origin. Further away from the blow out site, lower concentrations were found that had either a biogenic (methanogenesis) or a thermogenic signature.

2.3 BORZĘCIN (POLAND)

The Borzęcin natural gas reservoir has been producing gas since the 1970s. From initial production, the field produces sour natural gas containing hydrogen sulphide (H_2S) and carbon dioxide (CO_2). In the 1990s, after depletion of the gas reservoir, the Borzęcin site was used for acid gas injection and storage. Injected through one well (B28), the acid gas is injected in the saline water aquifer underlying the depleting gas reservoir (Figure 5) (e.g., Stopa et al., 2017; Stopa et al., 2006).

For the SECURe Project, the Borzęcin Field has been mainly studied for feasibility and safety of CO_2 re-injection. The natural gas reservoir is located in the Zielona Góra Basin, in the Polish part of the European Permian Basin. The reservoir is within the Rotliegend sandstones and Zechstein carbonates and is capped by the Zechstein evaporites (Karnkowski, 2007). Gas generation is proposed to be from the Carboniferous organic deposits with later migration into the Permian. At the Jurassic/Cretaceous boundary the south-western basin part was uplifted and intensively eroded (Karnkowski, 2007). The current reservoir temperature is 48.6 °C and reservoir depth is about ~1300m b.g.l. (Lubaś et al., 2020).

Figure 2: A. Rochasson (ROC) sampling site. Orange square=sample ROC 1 (main vent), purple triangle=sample ROC14 (soil sample). See Figure 1A for location of the Rochasson site. B. Sampling equipment at the main vent (ROC1). C. Soil flux measurements (blue dots) with location of the collected gas samples (see SECURe Report D3.4, 2021 for results). Note that map is rotated 90° to align with photo in A.

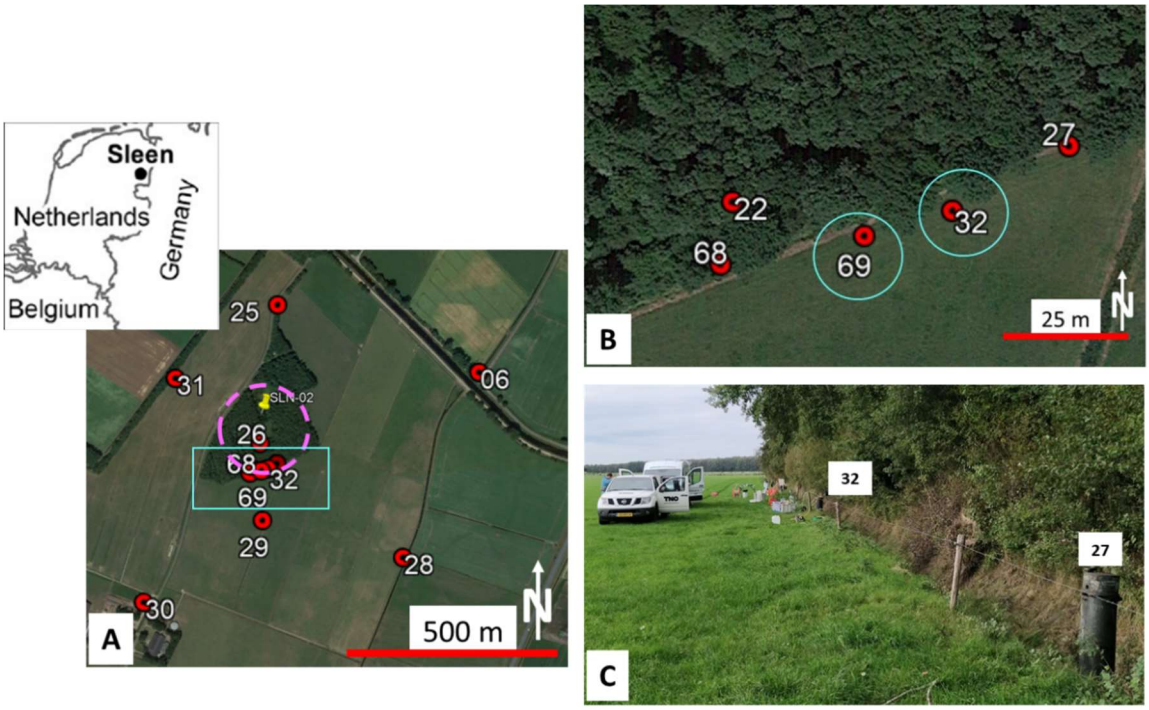

Figure 3: A. Location of the Sleen blow out site with groundwater monitoring wells. B. Close up of the well locations near the blow out site (turquoise box in A). C. Photo of the groundwater wells heads.

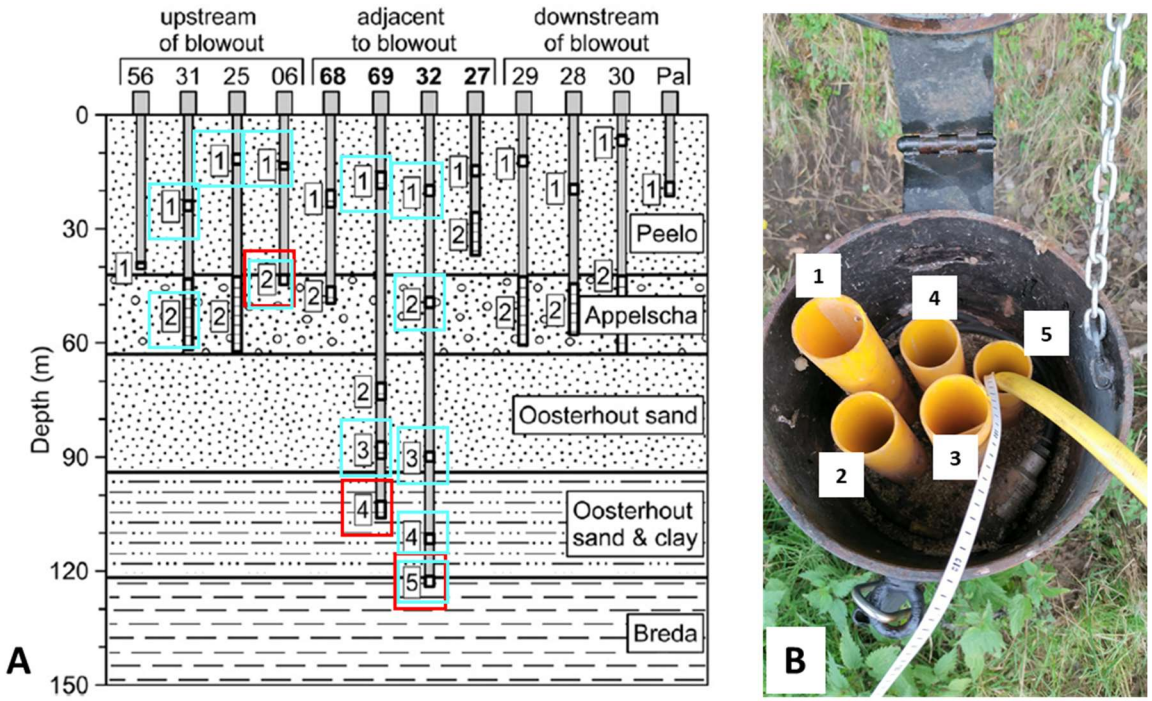

Figure 4: A. Schematic cross section of the shallow subsurface stratigraphy with the main formations and their dominant lithology (adopted from Schout et al., 2018). For each groundwater monitoring well, the approximate depth of the individual monitoring screen is provided. Red boxes depict the screes sampled for methane clumped isotope analyses; blue boxes for microbial analyses. B. Photo showing monitoring wellbore 32 with the 5 well tubes for each screen (with screen 5 being water sampled).

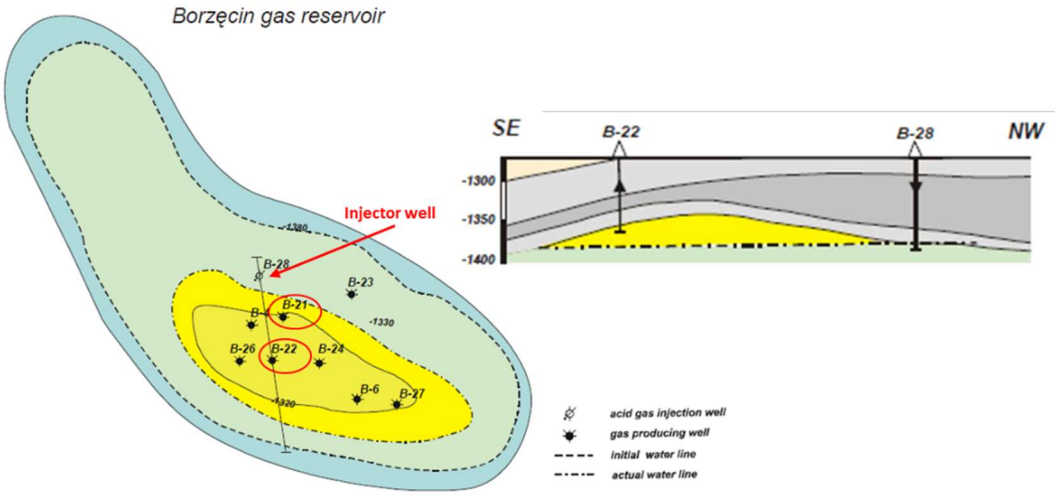

Figure 5: Map of the Borzęcin natural gas reservoir (modified from Stopa et al., 2017; Stopa et al., 2006). Red circles indicated the two wells (B21 & B22) sampled for methane gas.

3 Gas based sensors

3.1 CLUMPED ISOTOPE METHODOLOGY

Determining the origin of methane and/or CO_2 gas is routinely conducted by analysing their isotopic composition, in particular via the $\delta^{13}C$ ($^{13}C/^{12}C$) and δD (D/H) ratios (e.g., Schoell, 1980). There is however, some ambiguity as these ratios can overlap and do not provide a clear distinction between methane gas that has a thermogenic source (e.g., from hydrocarbon source rocks) or a biogenic origin (e.g., Young et al., 2017 and references therein).

A novel isotope tracer technique was tested for determining the source and origin of methane (and carbon dioxide) seeping to the surface. The method, generally referred to as Clumped Isotopes (CI), allows for the reconstruction of the temperature at which rocks, minerals or gasses are formed or precipitated. Initially developed to determine accurate (within 2-3°C) calcite/carbonate precipitation temperatures (e.g., Eiler, 2007; Eiler et al., 2014), recently clumped isotopes have been used to determine methane gas formation temperature (e.g., Stolper et al., 2014a; Stolper et al., 2018; Young et al., 2017).

The CI methodology is based on the bonding (or clumping) of the heavy isotopic bonds in a crystal lattice or gas. In carbonate minerals ($CaCO_3$), the C and O ions are primarily composed of ^{12}C and ^{16}O as they make up about 98% of the C and O isotopic composition ($Ca^{12}C^{16}O_3$, e.g., Eiler, 2007). A small portion, however, is composed of heavier isotopes ("isotopologues"), whereby a single (e.g., $Ca^{13}C^{16}O_3$) or multiple isotopes (e.g., $Ca^{13}C^{18}O^{16}O_2$) are substituted in the crystal lattice. For carbonate clumped isotopes, the degree of clumping of the ^{13}C and ^{18}O isotope bonds (expressed as Δ47, the atomic mass of the CO_2 molecule in the carbonate mineral consisting of the heavy isotopes $^{13}C+^{18}O+^{16}O$ = Δ47) versus a random (stochastic) distribution of isotopes is a direct proxy for the paleo-temperature at which the carbonate mineral formed.

In methane, a similar clumping of heavier isotopes is possible (e.g., Stolper et al., 2014a; Stolper et al., 2018; Young et al., 2017). About 98% of methane is composed of $^{12}CH_4$ (with H being the ^{1}H isotope of hydrogen). However, occasionally single or multiple substitutions occur whereby heavier isotopologues are formed (e.g., $^{13}CH_4$ or $^{13}CH_3D$, whereby D (deuterium) is the ^{2}H isotope of hydrogen). Also in methane, the clumping of these heavier isotope bonds is a direct proxy for the temperature at which the methane gas formed (e.g., Stolper et al., 2018). Annotation is analogue to carbonate clumped isotopes, and expressed as Δ18 for the degree of clumping of the heavy isotopologues versus a random (stochastic) gas distribution. For methane there are two isotopologues that comprise the Δ18: $^{13}CH_3D$ and $^{12}CH_2D_2$, denoted as $\Delta^{13}CD$ and ΔDD respectively. When in isotopic equilibrium the isotopologues provide the formation temperature of methane and thus pinpoint the formation process of the methane (Figure 6).

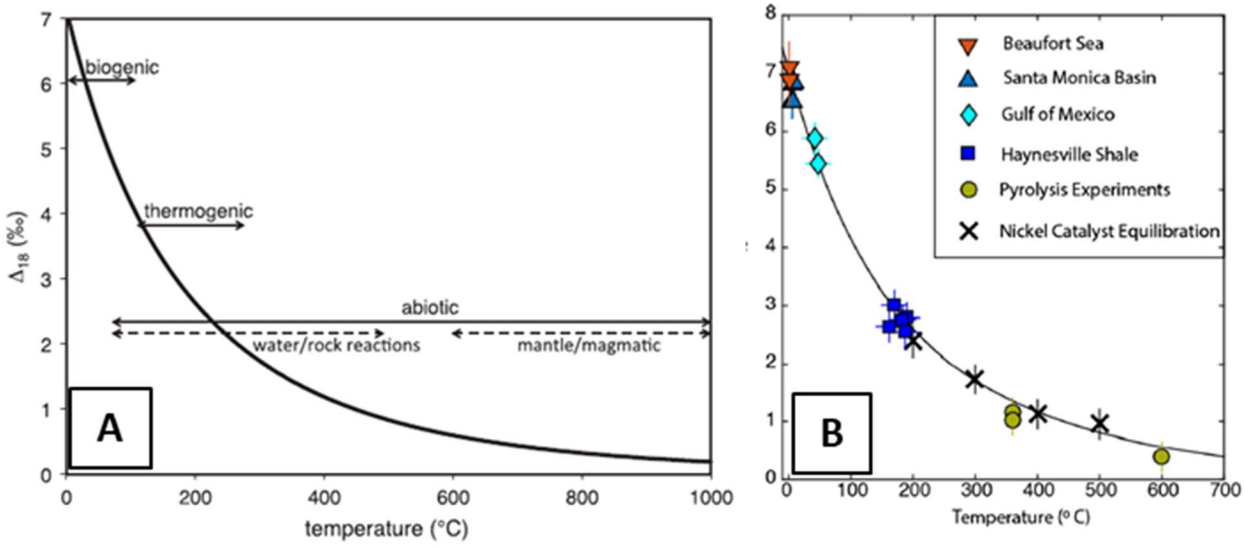

Figure 6: A. Theoretical calculation of equilibrium temperature dependence of Δ18 for methane generated from various reaction mechanisms (Stolper et al., 2014a). B: The relationship between Δ18 values and formation temperature for methane formed in internal isotopic equilibrium (Douglas et al., 2017).

3.2 CARBON-14 METHODOLOGY

The application of tree-ring dating in combination with isotope analyses has been postulated to serve as a monitoring tool for (past) CO_2 emissions (e.g., Cook et al., 2001; Donders et al., 2013). In living trees, tree rings form annually and integrate CO_2 concentrations over the course of the growing season resulting in a temporal averaged CO_2 signature (e.g., Cook et al., 2001). The trees take up CO_2 from air but in the presence of other CO_2 sources (e.g., from magmatic gas emissions or hydrocarbon leakages) trees and plants may incorporate part of this local CO_2.

Part of the carbon in the CO_2 taken up by the trees will be in the form of the Carbon-14 isotope. Present-day atmospheric CO_2 contains relatively high ^{14}C concentrations, which predominantly result from atmospheric nuclear bomb testing (e.g. Levin et al., 1994). In contrast, CO_2 emitted from magmatic or hydrocarbon sources will not contain Carbon-14 (^{14}C) as ^{14}C is radioactive (with a half-life of about 5.7kyr) and will have decayed. This ^{14}C depleted CO_2 is often referred to as “dead carbon”. Trees can take up this dead carbon and incorporate it into the wood. Consequently, deviations of the ^{14}C concentration relative to the mean atmospheric composition ($\Delta^{14}C$) can be used to detect seepage extent, temporal variability, and time of onset (Donders et al., 2013).

Challenges in this method lie in determining the distances from the CO_2 point source to the trees that incorporate the dead carbon, determining prevailing (historic) wind directions and statistical number of analysed samples.

3.3 SAMPLE COLLECTION

3.3.1 French Alps and Borzęcin field sites

3.3.1.1 GAS SAMPLING

Two duplicate natural gas samples were collected from the Borzęcin gas reservoir from wells B21 and B22 (Figure 5, Table 1). The sampling was conducted by INIG in May 2019. The samples were taken from gas metering lines at the surface installation and directly transferred to the 1L gas-tight glass vessels at pressures of 2.26 MPa for well B-21 and 2.50 MPa for well B-22. The sample vessels were initially flushed with 3 volumes of reservoir gas. The gas was sourced from reservoir depth of 1435m for well B-21 and 1419m (b.g.l.) for well B-22. Subsequently the samples were shipped to the Netherlands for isotope analyses.

Terrestrial gas sampling at Fontaine Ardente and Rochasson was performed by inserting a soil probe or burying an inverted funnel over an active gas vent (Figure 1, Figure 2 and Table 1). The gas was pumped slowly from the gas vent into 1L gas-tight glass vessels through a drying agent filled with $Mg(ClO_4)_2$. The vessel was flushed with 3 volumes of gas before it was collected. Samples FA65 and ROC1 were sampled directly at the main gas vents, whereas FA29 (an ROC14) were sampled in the vicinity of the main gas vents from soil gas. Sample FA03 and RO-01 and RO-02 were collected in Isotubes that were flushed 3 times prior to sample collection. In order to reduce water content, the gas was flowed through a 5mm diameter coiled copper tube that was held in an ice bath (with added salt) at ~-15°C. Samples FA03 and RO-01 were collected by placing a funnel directly over the vents and connecting this to the Isotube; sample RO-03 was collected via an ~1.5m long copper tube directly inserted into the soil.

3.3.1.2 TREE RING SAMPLING

BRGM tested ^{14}C activities and stable carbon isotope ratios of tree rings and herbal vegetation in the proximity of the FA field site. Wood samples were taken from two alder trees, at different distances and directions from the main gas vent. Grass leaves and roots (*Carex* sp.) were analysed for two spots with different soil methane concentrations and fluxes within the zone of diffuse gas emanation around the main vent (Gal et al., 2019). Grass and wood samples show contrasting isotope compositions depending on their species, age, and position with respect to the gas seep, some with ^{14}C activities significantly lower than present day values.

3.3.2 **Sleen field site**

3.3.2.1 DEVELOPMENT OF GROUNDWATER SAMPLING SYSTEM

Several methods exist for sampling groundwater and dissolved gasses (e.g., glass containers, sample bags such as Isoflasks). Provided that a cannister or Isoflask is not filled to spill, the gas will dissolve from the groundwater and reside in the headspace from which it can be sampled for (isotope) analyses. Samples collected in this way can be stored for up to several months (in a fridge) without the risk of sample degradation. To prevent bacterial degradation of the water sample, water must be filtered prior to collection or have a pre-inserted bactericide capsule such as in Isoflasks.

A challenge in the above-mentioned sampling methods is that the volume of the groundwater sample is limited. Especially for the methane clumped isotope analyses, high methane concentrations (preferable > 40% methane gas) are required. Therefore, when sampling groundwater with low methane concentrations, significant volumes of water are needed in order to degas sufficient methane for sample analyses.

A new sampling system was constructed to allow for the collection of tens of litres of groundwater. Whereas large volume sampling containers are readily available, they need to be thoroughly leak tight against gas escape, hence single walled water containers with screw tops are not suitable. Instead, a sampling set up was developed using plastic containers (Figure 7). The containers (KeyKeg, Den Helder, The Netherlands) are composed of double layered plastic with a (re-)fillable aluminium lined airtight vacuum bag that is able to hold 10, 20 or 30L. The main advantage of this setup is that the double walled container with the airtight bag is compartmentalised, hence the container space between the plastic outside vessel and the sampling bag can be pressurised. This allows for the gas to be dissolved in the groundwater under aquifer pressure conditions when sampling the water (Figure 7).

The sample cannister has two valves (Figure 7C). Valve 1 is used to pressurise the container (max 4 bar). During sampling, valve 1 is used to slowly vent the pressured cannister and the pressure gauge is used to maintain a required minimum pressure to keep the gas dissolved in the groundwater (2.5 – 3 bar during sample collection). The sample inlet is connected to the groundwater sampling pumps. A second valve is connected in order to flush the contraption prior to groundwater sampling.

Table 1: Gas compositions of the sampled gas from the natural gas seepage sites in the French Alps (Fontaine Ardente (FA) and Rochasson (ROC)). bd= below detection, nd=not determined; na=not available.

Sample	CH4 (vol%)	C2H6 (vol%)	C3H8 (vol%)	N2 (vol%)	CO2 (vol%)	H2 (vol%)	H2S (vol%)	He (vol%)	O2 (vol%)	Ar (vol%)	C1* (vol%)	C2* (vol%)	C3* (vol%)	N2* (vol%)	CO2* (vol%)	Air correction	δ13C-CH4 ‰ (PDB)	δD-CH4 ‰ (SMOW)	δD-ethane ‰ (SMOW)	δD-propane ‰ (SMOW)	δ13C-CO2 ‰ (PDB)
French Alps fieldsite																					
FA49[#]	21.9	0.011	nd	59.8	1.6	nd	nd	nd	16	0.72	93.3	0.048	0.0003	0	6.7	corrected for 76.5% air	-27.2	-146	nd	nd	-7.0
ROC 1a[#]	81.3	1.6	0.25	12.9	0.27	nd	nd	nd	3.5	0.16	97.3	1.9	0.3	0	0.32	corrected for 16.5% air	-34.6	-152	nd	nd	-10.9
ROC14[#]	0.12	0.0082	0.0044	79.6	0.77	nd	nd	nd	18.6	0.94	1.1	0.075	0.04	91.7	7.1	corrected for 89.1% air	-12.8	-37	nd	nd	-35.1
FA 65[§]	87.0	nd	nd	1.02	9.5	0.04	0.02	0.02	0.274	0.012	88.1	na	na	0.00	9.6	unknown	-28.3	nd	nd	nd	-12.0
FA 29[§]	0.31	nd	nd	78.4	0.31	bd	0.00	0.01	20.4	0.92	nd	nd	nd	nd	nd	unknown	-25.3	nd	nd	nd	-18.8
ROC 1[§]	74.1	nd	nd	17.6	0.84	0.02	0.18	0.007	4.4	0.197	94.7	na	na	1.08	1.07	unknown	-35.0	nd	nd	nd	nd
FA65[&]	na	na	na	na	na	na	na	na	na	na	na	na	na	na	na	unknown	-30.7	-137	nd	nd	-8.8
ROC 1[&]	na	na	na	na	na	na	na	na	na	na	na	na	na	na	na	unknown	-35.1	-138	nd	nd	-7.1
Borcezin fieldsite																					
B-21[@,§]	66.2	2.0	0.3	31.0	0.33	nd	nd	nd	0.012	0.016	66.3	2	0.3	30.9	0.33	corrected for 0.13% air	-34.6	-115.9	-30.2	-26	-12.4
B-22[@,§]	65.6	2.0	0.3	31.0	0.79	nd	nd	nd	0.0052	0.016	65.7	2	0.3	31	0.79	corrected for 0.098% air	-34.4	-117.8	-30.2	-26.4	-13.9

* recalculated to atmosphere-free contents, based on the oxygen content

[#] gas composition and isotope analyses conducetd at Isolabs, The Netherlands

[§] gas composition and isotope analyses conducetd at GFZ, Germany

[&] $\delta^{13}C$ and δD isotope data from BRGM, see SECURe deliverable D3.4

[@] gas composition analyses conducted at Isolabs, The Netherlands

[§] $\delta^{13}C$ and δD isotope data from Oil and Gas Geochemistry Laboratory of INiG-PIB, Poland (Lubaś et al., 2020)

Figure 7: A. Photo of the double walled sampling container with the sampling bag. B. Detailed photo of the sampling valves. C. Schematic drawing of the sampling setup. Compressed air inlet is used to pressurise the container with valve 1 and pressure gauge for depressurisation. Sample inlet is connected to the pumps collecting the groundwater and has a second valve that allows to flush sampling valves prior to sample collection.

3.3.2.2 SLEEN GROUND WATER SAMPLING

Wells were sampled by a combination of peristaltic and Grundfuss pumps. Each well was purged for at least three well volumes prior to sampling to ensure that all the groundwater in the wells were flushed.

Large volume groundwater sampling from three Sleen wells used the setup discussed in Section 3.3.2.1. Owing the smaller molecular structure of methane compared to CO_2, methane is likely to be more prone to leakage from the groundwater sampling bag. Hence, initial testing of the developed setup was conducted by degassing methane from the groundwater in standard and accepted sampling bags (Isoflasks). The isotopic composition of the gas in the headspace was analysed and compared to degassed groundwater in the large volume cannisters (see Section 3.5.2).

Two sampling campaigns to the Sleen site were conducted. In November 2019, groundwater/gas samples were collected from five wells (Table 3). Based on historic gas composition data, two wells were considered to have the highest methane concentrations with a thermogenic origin (32 and 69, Schout et al., 2018) whereas one well (06) was expected to have the highest biogenic methane concentrations. Two additional wells (25 and 31) were sampled to assess regional temporal changes in methane concentrations related to the former blowout site. In each of the wells, groundwater plus dissolved gasses were collected from multiple depth screens (Table 3) in Isoflasks. Gas composition and isotopic data were determined on all collected samples (Table 3). The wells (and depth screens) 32-05, 69-04 and 06-02 were sampled for methane clumped isotope analyses. To prevent bacteriological degradation of the collected groundwater samples, all the water was passed through a 0.45μm mesh size filter prior to collection. All water samples were brought to room temperature (~20°C) prior to methane degassing.

In order to test the suitability of the large water sampling set up, well 69-04 was used to test various sampling and degassing techniques. One sample was collected using a conventional Isoflask (~300ml) and considered the benchmark (sample 69-04_isoflask, Table 3). Two large volume (30L) water samples were collected in the KeyKegs for testing methane degassing techniques. One large volume water sample was passed through a membrane contactor (Reichel, 2013) to extract the gas from the groundwater. In this set up full separation between the gas and liquid phase is achieved. The extracted gas is then collected in a high vacuum all metal cannister and the isotopic composition was determined (sample 69-04_contactor, Table 3). A second large volume water sample was degassed by simply depressurising the KeyKeg to atmospheric conditions and slowly allowing methane to dissolve for few hours. The headspace gas in the KeyKeg bag was then transferred to an all-metal vacuum cannister and its isotopic composition was determined (sample 69-04_keykeg, Table 3). Isotopic compositions determined for all three different techniques are identical suggesting that at least for the conventional isotope analyses, the different degassing techniques work well (Table 2). The membrane technique, however, may result is isotopic fractionation for the rare, heavy isotopes ^{13}C and ^{2}H which are

measured in the clumped isotope method (Popa (2020), pers.comm). It was therefore decided that degassing through depressurising the KeyKeg was the preferred method for degassing the methane gas.

The final workflow developed for degassing the samples involved overnight equilibration of the samples from ~6°C to room temperature (23°C), followed by removal of the overpressure in the outer container. Pressure release results in near instant dissolution of methane from the groundwater. The containers were allowed to degas for few hours to ensure near complete dissolution. The headspace gas was then transferred into 6L high vacuum all metal cannisters and transferred for gas analyses.

Following degassing of the November 2019 samples and transfer to the all-metal high vacuum cannisters, helium was added to increase the pressure and allow for flow from the cannister to the methane clumped isotope gas purification line. This proved to have an adverse effect on the methane purification as the helium hampered flow of the methane gas through the extraction line resulting in incomplete methane separation.

A second sampling campaign was set up in October 2020 during which three new large water samples were collected for wells 06-02, 32-5 and 69-4. 30L vessels were filled from wells 32-5 and 69-4, whereas 120L was collected for well 06-2. Small water volumes (~300ml) were collected for isotopic composition analyses for comparison to the methane clumped isotope data and smaller groundwater samples were collected for standard chemical analysis.

3.4 DATA ACQUISITION

3.4.1 Gas analyses

For the Borzęcin site conventional isotopic composition of stable carbon and hydrogen isotopes in CO_2 and CH_4 (C1 - C3) was measured in the Oil and Gas Geochemistry Laboratory of INiG-PIB on a Delta V Advantage Isotope Ratio Mass Spectrometer. Major gas composition of the FA and ROC samples was measured on a gas chromatograph at GFZ. Carbon isotopes ($\delta^{13}C$) of CH_4 and CO_2 for FA and ROC were measured on a MAT 253 GC-IRMS at GFZ.

Gas compositions of B21, B22, 69-4a, 32-5a and 06-02a were analysed at Isolab B.V. in Neerijnen, The Netherlands. Natural gas composition is analysed on two GC's. H_2, O^2+Ar, N_2 and methane are analysed using an Agilent 6890N/7890A/7890B GC with TCD detector. Hydrocarbons and CO_2 are analysed on a separate Agilent 6890N/7890A/7890B GC equipped with a TCD detector (for CO_2) and a FID detector (for hydrocarbons). From the results of all three detectors, one complete composition is calculated. Carbon isotopes of methane are analysed with an Agilent 6890N GC interfaced to a Thermo Delta S IRMS. Methane isotopes (δD) are measured on an Agilent 7890A GC interfaced to a MAT 253 IRMS.

Methane clumped isotopes were analysed at the Institute of Marine and Atmospheric Research (IMAU) at Utrecht University, the Netherlands (see section 3.4.2)

3.4.2 Methane clumped isotope analyses

3.4.2.1 GAS EXTRACTION AND PURIFICATION

Methane gas was purified using a high vacuum line connected to a double column gas chromatograph (GC). Configuration of the gas extraction line is modified from Young et al. (2017). Pumped by a combination of turbo-molecular and diaphragm pumps, pressures in the line are at ~1e-7 mbar.

Samples are injected from the sample holders into the gas extraction line through an ultra torr connection directly from the canister or flasks. Sample gas is subsequently passed through the extraction line via various traps for gas purification. Initial collection of the sample gas is achieved by trapping the gas on silica gel held at liquid N_2. Helium carrier gas is then used to flush the sample gas from the silica gel trap to the GC while simultaneously warming the trap to ~60°C.The helium carrier gas plus sample is then passed over the first of the two GC columns. Held at 50°C, this allows separation of H_2, Ar, O_2 and N_2 from methane and other hydrocarbons. Passage of the gas through the second column separates CH_4 from C_2H_6, C_3H_8 and higher order hydrocarbons. GC peaks are identified using a TCD detector. Retention times of base-line resolved methane are around 37 minutes.

Table 2: Gas composition and isotope data of samples collected at Sleen, The Netherlands. bd= below detection, nd=not determined; na=not available

Nov 2019 data														
Sample	CH4 (mg/L)	C2H6 (mg/L)	C3H8 (mg/L)	N2 (mg/L)	CO2 (mg/L)	O2 (mg/L)	Ar (mg/L)	δ13C-CH4 ‰ (PDB)	δD-CH4 ‰ (SMOW)	δD-ethane ‰ (SMOW)	δD-propane ‰ (SMOW)	δ13C-CO2 ‰ (PDB)	$\delta^{15}N$ ‰ (vs. AIR N_2)
06-1	1.73	0.00	0.00	16.09	75.23	1.31	0.64	-63.1	-246	nd	nd	-22.1	0.3
06-2	4.84	0.00	0.00	18.39	40.82	0.23	0.62	-73.6	-237	-31.5	nd	-18.0	nd
25-1	0.29	0.03	0.00	26.22	138.76	0.67	0.60	-31.8	-163	-28.2	-28.9	-26.9	nd
25-2	1.21	0.14	0.01	32.07	18.18	0.17	0.72	-25.9	-127	-28.2	-29.1	-23.5	nd
31-1	0.08	0.01	0.00	13.65	196.92	4.67	0.57	-24.8	-109	-28.6	-30.2	-16.2	nd
31-2	0.07	0.01	0.00	35.39	13.00	0.30	0.73	-29.0	-139	-28.8	-30.1	-24.7	2.0
32-5a	67.50	3.49	0.16	71.52	4.89	0.68	0.40	-21.6	-116	-27.5	-30	-19.2	2.2
32-5b	97.72	5.04	0.23	112.89	4.93	0.91	0.60	-21.7	-118	-27.4	-30.1	-19.1	2.5
69-3	99.36	5.38	0.21	109.90	9.16	0.68	0.24	-21.5	nd	-27.4	-28.5	-23.6	nd
69-4 Isoflask	65.24	3.81	0.14	55.88	16.40	0.49	0.15	-21.4	-117	-27.2	-27.6	-23.5	3.0
69-4_contactor	nd	nd	nd	nd	nd	nd	nd	-21.3	-116	-27.1	-26.9	-26.4	2.5
69-4_keygeg	nd	nd	nd	nd	nd	nd	nd	-21.6	-116	nd	nd	nd	nd

Oct 2020 data													
Sample	CH4 (vol%)	C2H6 (vol%)	C3H8 (vol%)	N2 (vol%)	CO2 (vol%)	O2 (vol%)	Ar (vol%)	δ13C-CH4 ‰ (PDB)	δD-CH4 ‰ (SMOW)	δD-ethane ‰ (SMOW)	δD-propane ‰ (SMOW)	δ13C-CO2 ‰ (PDB)	$\delta^{15}N$ ‰ (vs. AIR N_2)
06-2	23.5	0.0	0.0	62.7	10.8	2	0.91	-74.6	-246	nd	nd	nd	nd
32-5	54.2	1.3	0.039	43.2	0.3	0.82	0.19	-21.4	-119	nd	nd	nd	nd
69-4a	59.4	1.9	0.053	35.6	1.1	1.9	0.13	-21.1	-118	nd	nd	nd	nd
69-4b	64.7	2	0.056	31.8	1	0.28	0.06	-21.1	-117	nd	nd	nd	nd

After passage on the second column, the purified methane gas is trapped on a second, liquid-N_2 cooled silica gel trap. In the final step, Helium carrier gas is first evacuated from the trap held at liquid-N_2 temperature and then the sample is transferred to an evacuated sample tube filled with silica gel by heating the trap to 60°C. This tube is subsequently connected to, and gas is introduced in the mass spectrometer by heating the silica gel to 60°C.

3.4.2.2 CALIBRATION GAS PROCEDURES/DEVELOPMENT

To reproduce the temperature calibration scale, methane was heated with activated Pt on Al_2O_3 for temperatures between 200 – 500°C and activated γ-Al_2O_3 for temperatures below 165 °C.

The quartz tubes with activated catalysts were evacuated to e-7 mbar and then filled with approx. 300 mbar of methane. These filled tubes were heated for specific durations corresponding to the desired temperatures. The heated gas was then extracted using our extraction line before introducing to the mass spectrometer. The temperature dependence of the obtained anomaly (between heated gas and cylinder gas) was compared to the calibration functions given in Eldridge et al. (2019).

3.4.2.3 MASS SPECTROMETRY

There are several analytical challenges when trying to determine the clumped isotopic composition of methane. These include the mass resolution when determining the rare isotopologues in methane as well as correcting for isobaric interference (e.g., Stolper et al., 2015; Stolper et al., 2014b; Young et al., 2017; Young et al., 2016). When determining routine bulk carbon and hydrogen isotopes of methane, methane is converted to CO_2 or H_2 when determining $\delta^{13}C$ and δD respectively. For clumped methane isotope measurements this approach is not possible and high-resolution mass spectrometers able to separate species on atomic mass 16, 17 and 18 are required (e.g., Stolper et al., 2014b; Young et al., 2017). Such resolving powers are for example required to discriminate between isotopologues on mass 17 (e.g., $^{13}CH_4^+$ and $^{12}CH_3D^+$) or determining interfering isobars (e.g., $^{17}O^+$ or $^{16}OH^+$ forming by separation from water, H_2O). Similar interferences and mass resolution are observed on mass 18 where the prime methane isotopologues $^{13}CH_3D^+$ ($\Delta^{13}CD$) and $^{12}CH_2D_2^+$ (ΔDD) are measured. Here, water ($H_2{}^{16}O^+$) is the most problematic as it is always present in a mass spectrometer in much higher concentrations than $\Delta^{13}CD$ and ΔDD.

At IMAU, bulk and clumped isotopic compositions are determined using a Thermo Scientific IRMS-253 Ultra (abbreviated to 'Ultra', Eiler et al., 2013). The Ultra has a mass resolution resolving power of 35,000 which is sufficient to separate methane isotopologues from each other and from contaminating isobars like H_2O^+, OH^+, NH_3^+, etc. Main isotopologues measured on the Ultra are $^{12}CH_4^+$, $^{13}CH_4^+$, $^{12}CH_3D^+$, $^{13}CH_3D^+$, and $^{12}CH_2D_2^+$.

Bulk isotopic compositions $\delta^{13}C$ and δD are directly determined using the ratios $^{13}CH_4^+/^{12}CH_4^+$ and $^{12}CH_3D^+/^{12}CH_4^+$ on mass 17; since these isotopologues can be distinguished on Ultra, the conversion to CO_2 or H_2 is not necessary. The mass spectrum on mass 18 includes measurements of species $H_2{}^{16}O^+$, $^{13}CH_3D^+$, and $^{13}CH_5^+$ (and rarer isotopologues) as well as possibly interfering species like $H^{17}O^+$, $D^{16}O^+$, $^{15}NH_3^+$ and $^{14}NH_4^+$. In the setup at IMAU, the isotopologues of interest ($^{13}CH_3D^+$, and $^{12}CH_2D_2^+$) are sufficiently separated from the interfering peaks, thus no corrections are necessary.

Each sample is measured in repeated acquisition cycles for a long time (about 20 hours), until all the gas is consumed. Each such acquisition includes measurements of the sample gas of a calibrated reference gas. The mean over these measurements is reported as the result for the sample; the typical standard error of the measurements is about 0.3 ‰ for $\Delta^{13}CD$, and 2-3 ‰ for ΔDD.

One of the samples was extracted and measured repeatedly in order to assess the overall reproducibility of the whole procedure. The variability of these measurements is within the overall measurement precision.

3.4.3 **Water analyses**

Temperature, pH, electrical conductivity and dissolved oxygen was measured prior to sampling (Table 3). 50ml of water was collected for major ion and cation analyses for each well (Table 4).

Sleen groundwater samples were analysed at Het Waterlaboratorium, Haarlem (The Netherlands). Analysis of trace metal and major cations was conducted with inductively coupled plasma mass spectrometry (ICP-MS) following the NEN-EN-ISO 17294-1 and NEN-EN-ISO 17294-2 standards.

Table 3: Sleen groundwater chemical data at sampling.

Well/screen	Depth (m)	Formation	CH4 mg/L	C2H6 mg/L	C3H8 mg/L	pH	Conductivity uS/cm	Oxygen %
6.2	-40	Appelscha	5.2	0.001	0.003	6.8	392	1.6
32.5	-119	Breda	36.9	2.16	0.099	8.1	1698	1.0
69.4	-100	Oosterhout				7.5	540	0.25

Table 4: Major ion and cation concentration in Sleen water samples

Sample	*32-5*	*69-4*	*06-2*
Element	Concentration (mg/L)	Concentration (mg/L)	Concentration (mg/L)
N	0.62	0.18	0.11
NH4	0.8	0.23	0.15
Ca	25.1	56.12	29.67
Cl	345	41	39
K	11	2.97	0.93
Mg	8.5	6.12	2.48
Na	241	35.6	28.5
N	<0.20	<0.20	<4.0
NO3	<0.89	<0.89	<17.8
SO4	<2.0	<2.0	<2.0
Fe	0.346	3.17	18.8
Mn	0.069	0.039	0.527
Al	0.0076	0.0041	0.0043
As	0.0009	0.0006	0.0007
Zn	0.0262	0.0052	0.003
DOC	2.52	1.12	10.1
pH	7.09	7.85	6.73
°C	17.2	17.1	17.3

3.5 RESULTS

3.5.1 Gas compositions

At the French Alp sites the main component of the gas vents is methane, followed by CO_2 and N_2. C2+, H_2S, He and H_2 are minor gas species (Table 1). Fontaine Ardente gas is a CO_2-rich site (~10 vol%), whereas Rochasson gas is CO_2-poor (~1vol%). The wet gas components (C_2H_6 and C_3H_8) are between 0.6 and 2 vol% (Gal et al., 2017). Although precautions were taken not to include atmosphere in the samples, a small amount was present in the vessels as can be identified by the oxygen content. The concentration of the main gas vents was thus recalculated to deduct contribution from the atmosphere.

The Borzęcin reservoir gas is with ~ 67 vol% far lower in its methane content but exceptionally rich in N_2 (~ 30 vol%, Table 1). The wet gas content is ~ 2 vol% (Lubaś et al., 2020).

Gas composition of the Sleen wells is dominated by methane (~50 vol%) followed by N_2 (30-60 vol%). Minor components include CO_2 (up to 10 vol%) and O_2 (up to 2 vol%), Table 2. Wet gas components are between 1-2 vol% for C_2H_6 and ~0.05 vol% for C_3H_8. Oxygen corrections to account for the possible atmospheric O_2 are applied.

3.5.2 Isotope compositions

3.5.2.1 Bulk isotope data

The conventional isotopes composition of the French Alp gases collected from the main and side vents range from -27 to -35 ‰ for δ^{13}C-CH_4 and from -137 to -152 ‰ for δD-CH_4 (Table 1, Figure 8). Carbon isotope values from these samples range between -7 and -11 ‰. The one soil sample ROC14 for which all isotopes are measured (for FA65 only δ^{13}C-CH_4 are available) has methane δ^{13}C and δD of -13 ‰ and -37 ‰ respectively. Carbon isotope value for this sample is significantly more depleted at -35 ‰.

The conventional isotope composition of the Borzęcin reservoir wells (B21 and B22) have similar values with -35 ‰ δ^{13}C-CH_4, and -119 ‰ δD-CH_4. Whereas the carbon isotopes are quite similar to the French Alps the deuterium is somewhat heavier. For the δ^{13}C-CO_2 of the Borzęcin reservoir gas we refer to the values measured by INIG (Chapter 3, Lubaś et al., 2020), with values ranging from -12 to -14 ‰.

Isotopic composition of the Sleen gas (Table 3, Figure 9) ranges from -109 ‰ to -246 ‰ for the δD-CH_4 and -21 ‰ to -74 ‰ for the δ^{13}C-CH_4. δ^{13}C-CO_2 and δ^{15}N isotopes were measured on the November 2019 samples only and range -18 to -27‰ and 0.3 – 3.0 ‰ respectively.

Owing to the COVID pandemic, not all wells at Sleen could be sampled. Initially it was planned to test the methane clumped method on the three wells with the highest thermogenic and biogenic methane concentrations and subsequently sample lower concentration wells and wells with mixed bio-thermogenic isotopic signatures.

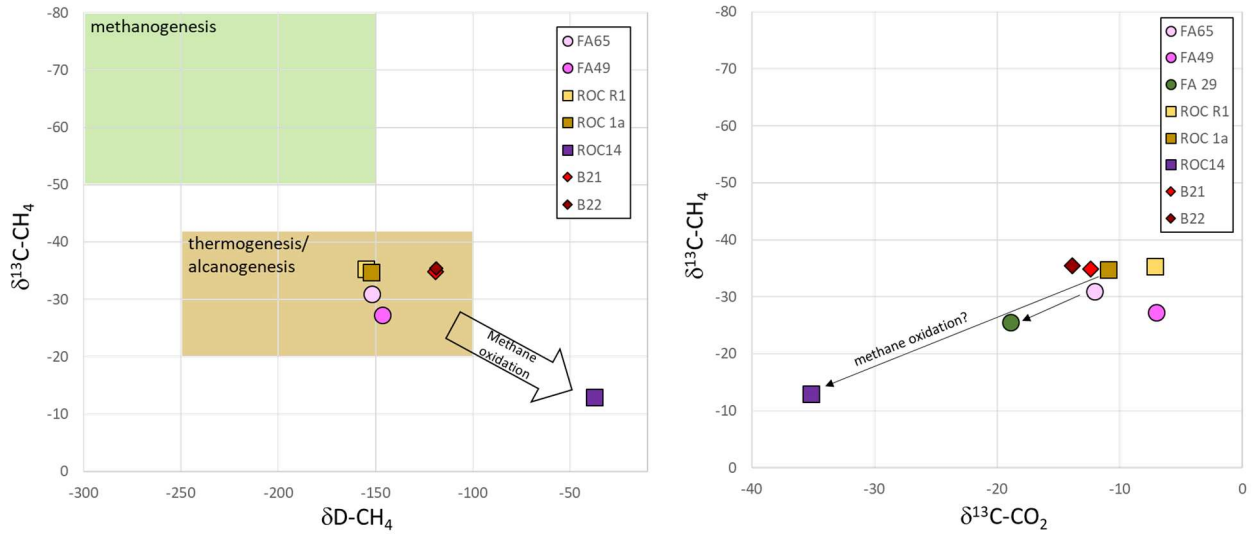

Figure 8: Isotope composition data for the natural gas seepage sites in France (Fontaine Ardente, FA and Rochasson, ROC)) and the natural gas reservoir of Borzęcin, Poland.

3.5.2.2 Methane clumped isotope data

Methane clumped isotopes range data were determined for Δ^{13}CD and ΔDD (Table 5 and Figure 10). Here reported are the clumped isotope data for samples from Borzęcin and Sleen. Data from the French Alps is currently restricted and not reported here as it is awaiting publication. Although duplicate samples were collected for both Sleen and Borzęcin, owing to the COVID pandemic it was not possible to have those analysed.

Initially it was also planned to conduct CO_2 clumped isotope analyses on FA and ROC samples (FA49, ROC14, ROC1a). However, they have a large air component (Table 1), hence any CO_2 clumped isotope gas

temperature would not yield the original gas formation temperature but (a mixture with) air CO_2. Due to the COVID pandemic it was not possible to conduct another sampling campaign to re-collect the samples.

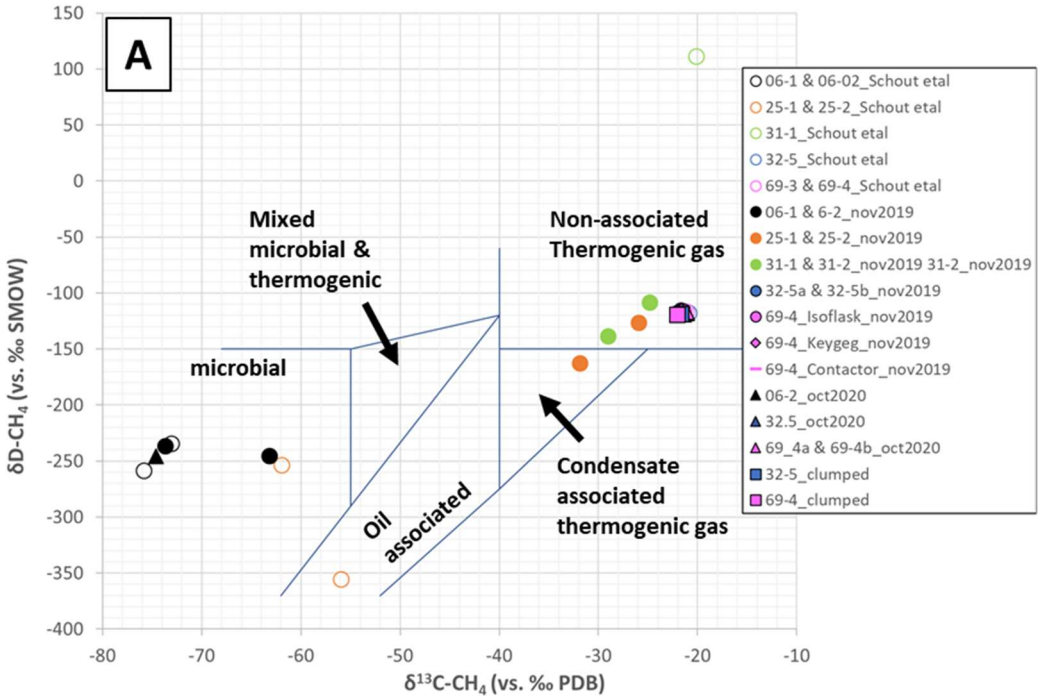

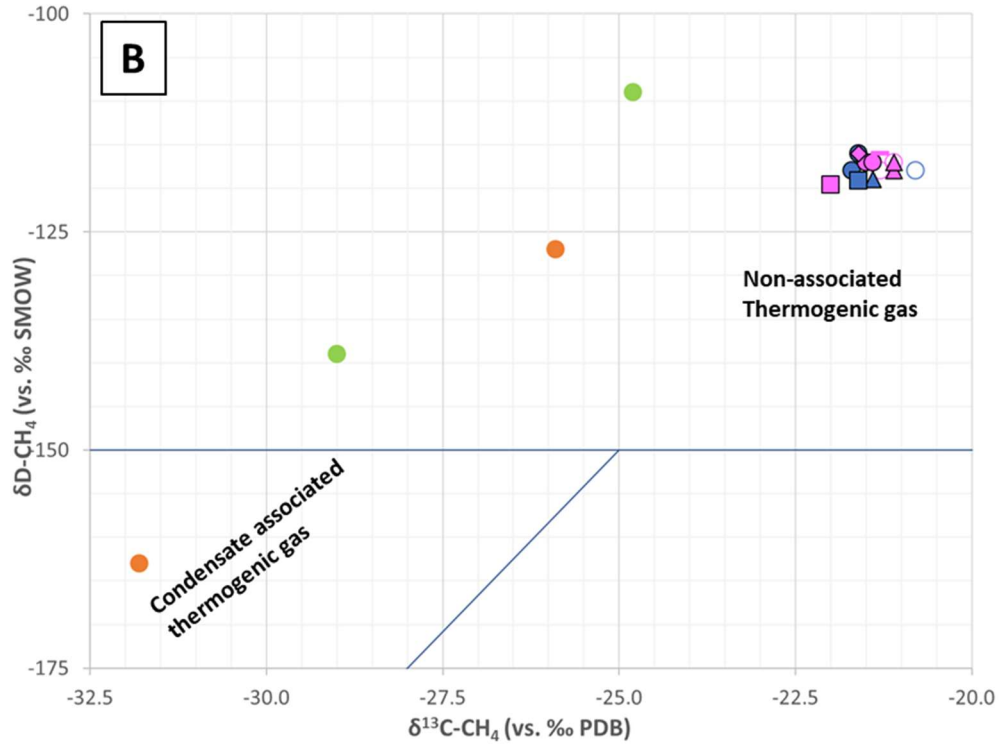

Figure 9: Isotope composition data for the Sleen wells. A. All sampled data. Historic isotope data from Schout et al. (2018) are depicted as open symbols; new isotope data are closed symbols. Compositional fields modified from (Schoell, 1980) and (Laughrey and Baldassare, 1995). B. Thermogenic samples (zoomed in). Isotopic data on samples (well 69, pink symbols) that were used to test the new sampling device, and different degassing methodologies (see text for discussion) are all indistinguishable demonstrating the robustness of the large volume groundwater testing setup.

Isotopic compositions ($\delta^{13}C$ and δD) are indistinguishable from bulk $\delta^{13}C$ and δD isotopes determined using established techniques (Table 5 , Figure 10). $\Delta^{13}CD$ and ΔDD values for the thermogenic Borzęcin and Sleen samples range between ~4.8 - 1.8 ‰ and 11 – 5 ‰ respectively. These data correspond to a gas formation temperature range ~65 to ~300°C (temperature calculated for both $\Delta^{13}CD$ and ΔDD, Table 5). Plotting the sample data in a $\Delta^{13}CD$ and ΔDD thermal equilibrium diagram (Figure 10) shows that with the exception of sample 69-04a, the data diverge slightly from the Thermal Equilibrium Curve (TEC). Deviation from the TEC likely indicates that mixing, isotope fractionation or diffusion processes may have affected the samples (e.g., Young et al., 2017).

Sleen sample 06-02 has $\Delta^{13}CD$ and ΔDD of 5.3 and -16.6‰ respectively. Plotting this sample in the $\Delta^{13}CD$ and ΔDD thermal equilibrium diagram (Figure 10) shows that this sample has a large depletion in ΔDD of up to ~25‰ relative to equilibrium. Calculated clumped isotope temperature yields ~55°C. This temperature, however, is considered unreliable as the gas is not in thermodynamic equilibrium. The gas has a biogenic origin (from the bulk isotopic composition) and microbial activity likely has affected the methane clumping (see section 3.6.2.1).

Samples from Poland (B21 & B22) deviate somewhat from the equilibrium line $\Delta^{13}CD$ values. Corresponding calculated temperatures are 63-66°C for $\Delta^{13}CD$ and 105-108°C for ΔDD. The offset in both samples is systematic, suggesting that the gas has been affected by a single process. The depleted $\Delta^{13}CD$ values may reflect some degree of mixing with a non-thermogenic gas source and the calculated temperature may therefore not reflect the actual gas formation temperature.

Table 5: Methane clumped isotope data for the Sleen and the Borzęcin samples; sample data from the French Alps are restricted and not reported here.

Sample	δ13C (‰)	δ13C se	δD (‰)	δD se	Δ13CD (‰)	Δ13CD se total	ΔDD (‰)	ΔDD se total
Well B21a	-34.9	0.01	-119.3	0.11	4.74	0.36	10.8	3.0
Well B22a	-35.4	0.01	-119.0	0.15	4.81	0.34	11.0	2.2
32-5a	-21.6	0.01	-119.1	0.10	1.59	0.28	6.0	2.1
69-04a	-22.1	0.01	-119.6	0.10	1.82	0.31	4.6	2.1
06-02a	-76.8	0.01	-248.9	0.21	5.26	0.5	-16.6	3.2

In the Sleen samples, isotopic equilibrium is present in sample 69-04a (Figure 10) yielding temperatures that are, within uncertainty indistinguishable at 282°C and 242°C for $\Delta^{13}CD$ and ΔDD respectively. Sample 32-05a lies slightly above the TEC and is enriched in ΔDD compared to equilibrium. This yields corresponding temperatures of 317°C for $\Delta^{13}CD$ and 199°C for ΔDD respectively. It is possible that this sample is affected by isotope fractionation. Given the close proximity of the two sampled wells (15m apart) and the similar mode of sampling and sample storage, it is unlikely that diffusional processes (e.g., Young et al., 2017) have affected one sample more than the other. The departure from equilibrium indicates that the calculated temperature for sample 32-05 is less reliable than for sample 69-04.

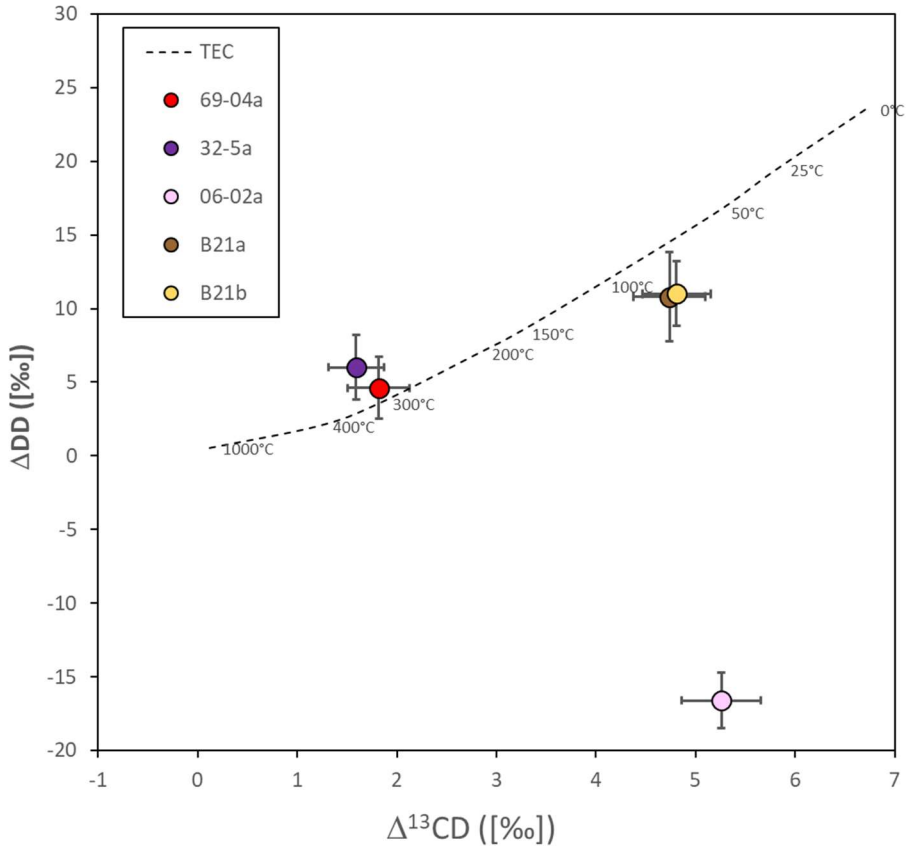

Figure 10: Clumped isotope data from methane gas samples collected from a natural gas reservoir (Borzęcin, Poland, samples B21 & B22) and a man-induced methane gas leakage site (Sleen, The Netherlands, samples 69-4 & 32-5). Data from the natural gas seepage (French Alps, samples F65, F65, R1) fall on the TEC but are not shown in this report due to peer reviewed publication in progress. TEC=thermal equilibrium line.

3.6 INTERPRETATION

3.6.1 Sleen

The isotopic composition of the Sleen gas samples indicate both a thermogenic (wells 32, 25, 31 & 69) and biogenic (well 06) gas origin (Figure 9). With the exception of well 25, these data are in line with historic gas analyses (Schout et al., 2018). For wells 32, 31 and 69, the data suggest that natural gas is still leaking from deep sources, likely the reservoir targeted by the exploration well. Although Schout et al. (2018) suggests that a deep reservoir origin is the most likely source for the gas, they discussed the possibility of lateral gas migration from secondary gas accumulations. Possibly even a shallow gas origin may be postulated which has been demonstrated to have occurred in The Netherlands offshore (e.g., ten Veen et al., 2011).

New isotope data from gas collected from well 25 (located to the NW of the original blowout site) suggest that at present, the gas in the groundwater has a thermogenic isotopic signature (Figure 9). Schout et al. (2018) observed that the gas had a biogenic origin. Although the actual gas concentration is still low (0.3 – 1.2 mg/L, Table 3), the shift in isotopic composition suggests that the gas plume may be spreading outward from the original drill site. Schout et al. (2018) noted that the groundwater flow is towards the south and the east. Well 25 is located upward from the groundwater flow, suggesting that the rising gas plume may be slowly spreading out rather than being carried by groundwater. Gas concentrations in well 25 are low, hence initially it was planned to collect large volume water samples (>150L) in order to conduct methane clumped isotope analyses. Owing to the COVID pandemic, and subsequent laboratory and office closures, it was not possible to have those samples analysed.

Nitrogen isotopes were measured on the Sleen blow out gas samples. $\delta^{15}N$ data on well 06 (n=1) suggest it has a (near) atmospheric composition. $\delta^{15}N$ isotopes on the samples from well 32 and 69 (Figure 11) suggest a thermogenic source originating from Westphalian coaly source rocks (Gerling et al., 1999; Gerling et al., 1997; Kotarba and Nagao, 2015). In the Dutch subsurface, coal intervals are present in various formations in the Carboniferous aged Limburg Group (DC, TNO-GSN, 2021).

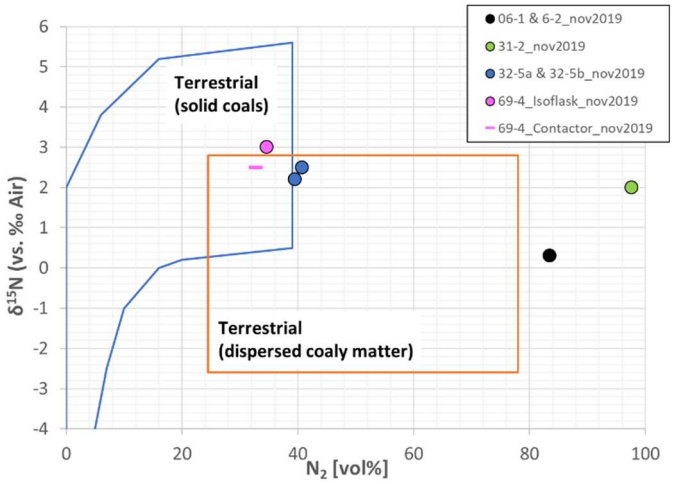

Figure 11: Nitrogen gas isotopes for the Sleen samples 32 and 69 suggest they have a Westphalian (coal) source rock origin (isotope fields from Gerling et al., 1997).

Regional 3D basin modelling studies have been conducted in the eastern part of the Netherlands (Nelskamp, 2011) and modelled formation burial temperatures can be used as independent constraints to reconstruct the origin of the Sleen gas and for comparing to the new methane clumped isotope gas formation temperatures.

A 1D modelled and calibrated well (GRL-01), located some 20km NW in the same basin structure as the Sleen wells, was extracted from the regional 3D model (Figure 12). Burial history and modelled temperature for Westphalian (Carboniferous) coaly and shaly source rocks in the Limburg Group (Maurits Formation (DCCU), Ruurlo Formation (DCCR), Baarlo Formation (DCCB) and Geverik Member (DCCGEG), TNO-GSN, 2021) suggest that they reached ~180°C for the Maurits Fm to ~230°C for the Geverik Mb in the Late Jurassic-Early Cretaceous. Modelled vitrinite reflectance data suggest that gas expulsion occurred from the Triassic onwards Figure 12B (NITG-TNO, 2000).

The maximum burial temperature modelled for the Geverik Mb is, within error, similar to the calculated methane clumped isotope temperatures for sample 69-04. This suggests that the gas leaking into the groundwater wells at Sleen indeed has deep source rock origin. From the methane clumped isotope data several other conclusions may be drawn. A large component of the measured Sleen gas seems to have been derived from the deepest buried source rocks as only these have modelled temperatures that match the calculated methane clumped isotope temperatures. In addition, comparing the modelled (maximum) burial temperatures to the gas formation temperatures may provide refinement of the timing of the main gas formation phase. Whereas previous modelling and vitrinite reflectance data suggest that gas expulsion started from the Triassic (NITG-TNO, 2000), the methane clumped temperatures suggest that main gas formation phase did not occur until source rocks reached temperatures > 220°C during the Late Jurassic-Early Cretaceous (Figure 12). Earlier gas formation may have occurred, but this may not have been trapped.

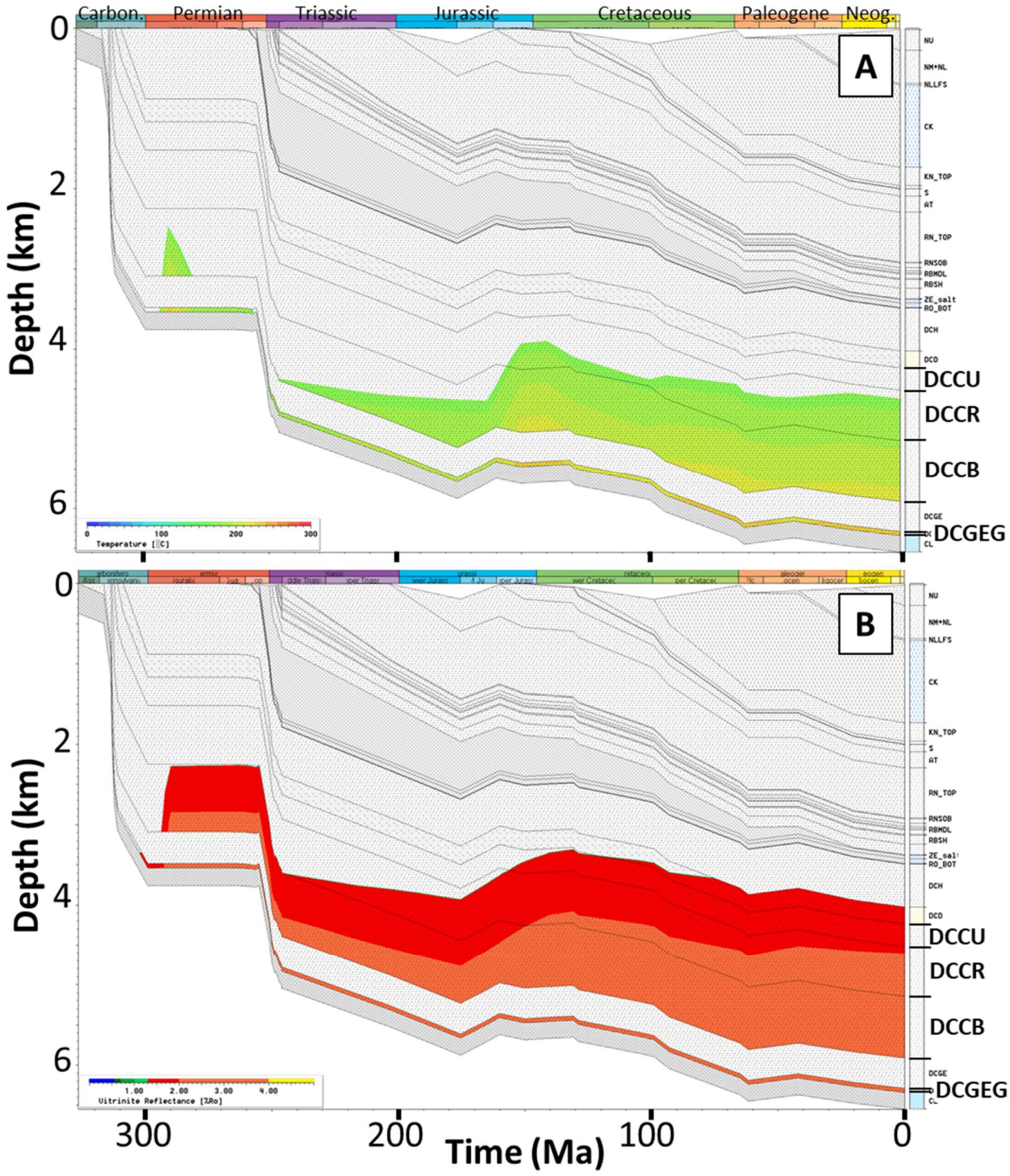

Figure 12: 1D well extraction (well GRO-01) from a regional 3D basin model for the Sleen region (Nelskamp, 2011). Relevant source rocks are Carboniferous coaly and shaly intervals in the Limburg Group: DCCU (Maurits Formation), DCCR (Ruurlo Formation), DCCB (Baarlo Formation) and DCGEG (Geverik Member) (TNO-GSN, 2021). A. Modelled burial temperature (depicted temperature range: 175-250°C). Modelled source rock temperatures reached ~180°C for the Maurits Fm to ~230°C for the Geverik Member at the Late Jurassic-Early Cretaceous. B. Modelled vitrinite reflectance data suggest that the source rocks reached the gas window from the late Permian – early Triassic onward.

3.6.2 French Alps and Borzęcin

3.6.2.1 GAS FORMATION AND ORIGIN

Methane δD-CH_4 and δ^{13}C-CH_4 values of the Borzęcin reservoir gas and the gas samples from the main seeps at FA and ROC suggest a thermogenic origin (Figure 8). At the French Alp sites, the samples ROC14 and FA29 were sampled in adjacent sites away from the main vent, where the methane concentrations are less than 1% of total gas. The δD-CH_4 and δ^{13}C-CH_4 in these samples do not fall into the thermogenic or methanogenic fields and are far higher (Figure 8). Although it is likely that methane derived from diffuse leakage from the same origin as the main vent, there is evidence that this methane has been largely oxidised. Compared to the main vents samples (ROC1 and FA65), δ^{13}C of CO_2 in the adjacent sites is shifted towards lower values (Figure 8). During methane oxidation the lighter carbon ventures preferably to CO_2 whereas the carbon in the residual CH_4 pool becomes heavier. This is equally the case for hydrogen. Particularly for sample ROC14 there is a large change in the CH_4/CO_2 ratio from 88.2 (main vent) to 0.15 as well as a lager difference in the isotope values.

Isotopologues from the main vents of Fontaine la Gua and Rochasson[(1)] fall on the thermal equilibrium line and indicate robust thermogenic temperatures.

In contrast to the findings provided by conventional isotopes (δD-CH_4 and δ^{13}C-CH_4) the isotopologue data from the Borzęcin gas reservoir does not indicate a classical thermogenic origin of the gas. The temperature of 63 to 66°C is much lower than thermogenic generation temperatures expected from Carboniferous source rocks. According to δD-CH_4 and δ^{13}C-CH_4 a microbial-methanogenic origin is also unlikely (see Figure 8). However, an admixture of abiotic gas cannot be discounted (Lubaś et al., 2020). Abiotic gas is formed mostly in disequilibrium and does not record true formation temperatures (Young et al., 2017). Mixing of a thermogenic and abiotic endmember could follow a mixing as described in Young et al. (2017), Figure 13. The source and formation of this abiotic gas is unknown but is likely low temperature abiotic formation.

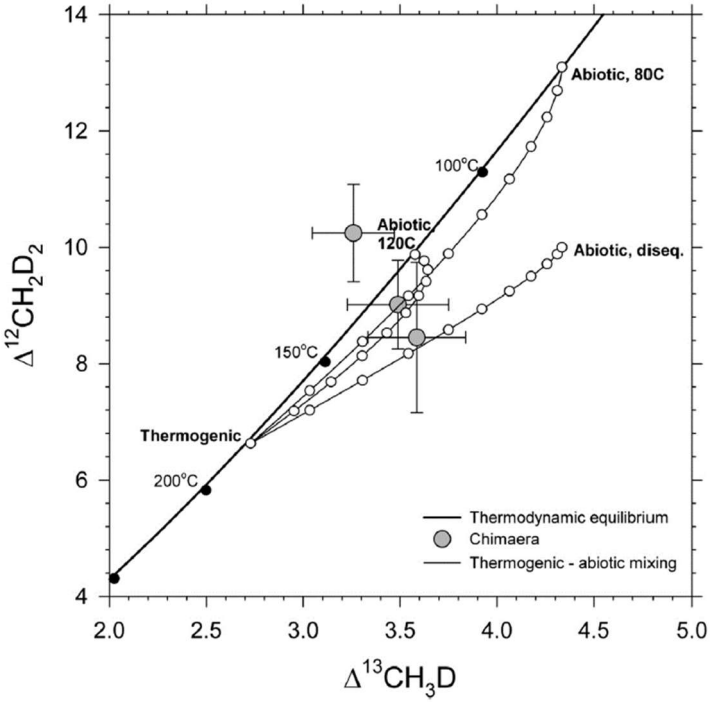

Figure 13: Mixing scenarios between thermogenic and abiotic gasses (Young et al., 2017).

Due to the high water-cut (Nm3/m3 = 0.6, Lubaś et al., 2020) and low pressure of the reservoir a foaming agent is used to force gas flow. Whether this process could have fractionated the isotopologues is unknown,

[1] Data not shown in this report, due to peer reviewed publication in progress.

however one would expect a variable amount of fractionation between the two wells, which is not the case as the $\Delta^{13}CD$ and ΔDD are identical within error.

Another conspicuous aspect is that the calculated temperature lies between the typical thermogenic generation temperature of 150 – 250 °C and the current reservoir temperature of 49°C, being closer to the present-day reservoir temperature. The question is whether the isotopologues may have been equilibrated over the time since the basin was uplifted and eroded in the late Cretaceous/Tertiary to the current temperatures. At this stage it is not possible the determine the actual source(s) with more certainty without further analyses.

3.6.2.2 CARBON-14 FOR LONG-TERM BASELINE MONITORING

Figure 14 shows that the radiocarbon activities of the alder tree upwind of the Fontaine Ardente (Alder 1) are mainly compatible with those measured on an old *Fagus Sylvatica* on the northern hemisphere (Lardie Gaylord et al., 2019) whereas alder two, situated downwind of the main vent has significantly lower ^{14}C-activities than would be expected for post-bomb atmospheric values. We interpret this as an integration of "dead" carbon from the CO_2 (direct emission or oxidized methane) transfer, via the atmosphere, of the natural gas seep.

The grass leaves and roots of *Carex sp.* growing within the diffuse methane emanation area around the main gas vent are significantly depleted in ^{14}C so that radiocarbon conventional ages are abnormally old (330 to 550 y before present). For these samples we observe also a depletion in ^{13}C (Figure 15). *Carex* has the ability to transfer methane from the root zone to the atmosphere. The strong ^{13}C-depletion of both leaves and roots analysed in the diffuse methane emanation zone could be related to the assimilation of thermogenic methane but other effects, notably methane oxidation, the influence of deep CO_2 from the geogenic gas seep and the associated carbon isotope fractionation processes have to be taken into account to explain these values.

So far, it can be stated that vegetation around a gas seep, in our case a natural analogue, has the potential to act as an integrator of gas emanation over time and, if tree rings are used, as an archive of gas fluxes. This offers perspectives of using vegetation carbon isotopes as proxies for present and past gas emanations, including man-induced gas leaks, e.g. from gas storage or natural gas exploitation facilities.

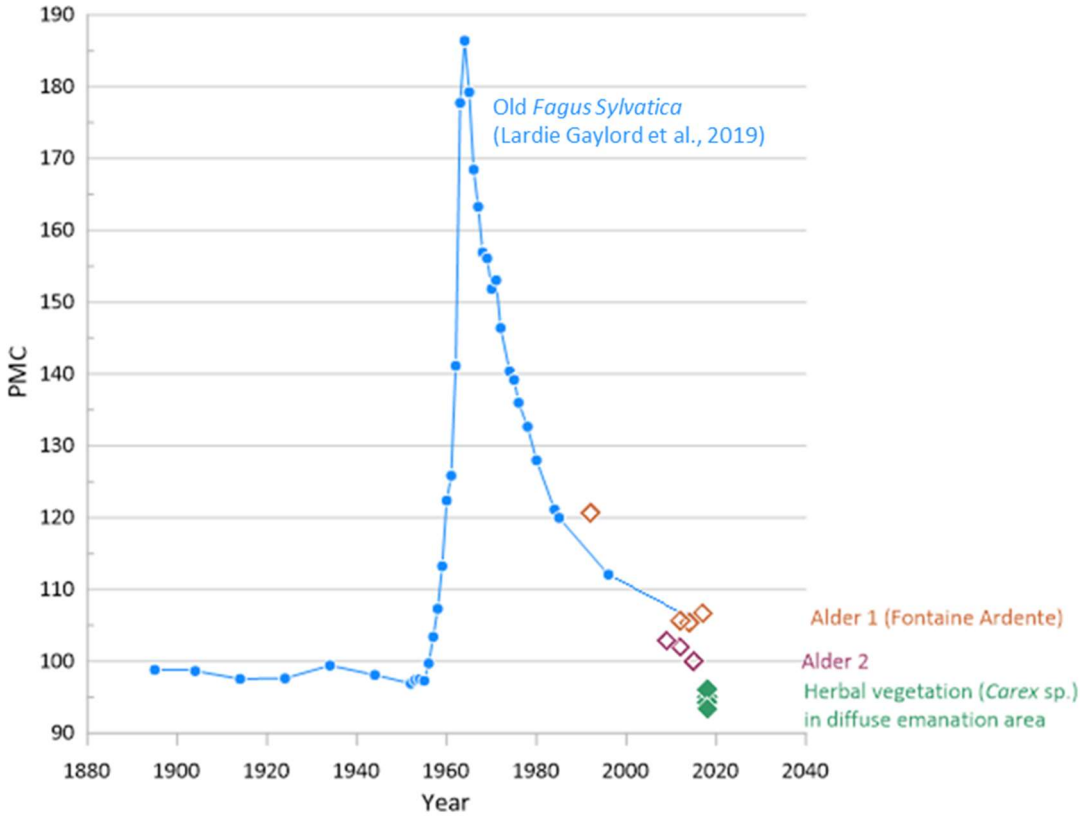

Figure 14: Preliminary data analysis of tree ring and herbal vegetation radiocarbon activities (tree ring counting to be confirmed).

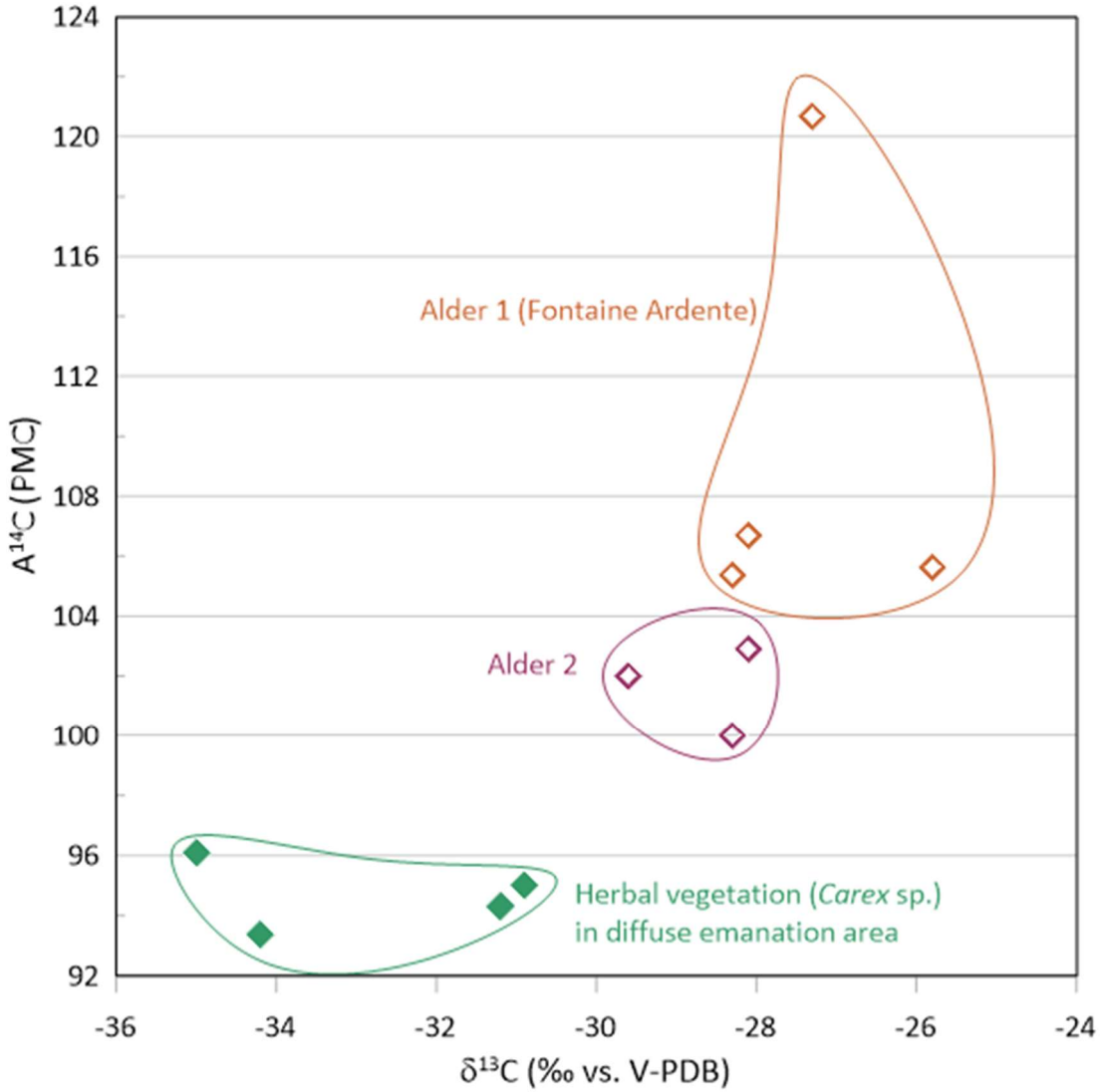

Figure 15: A14C vs. $\delta^{13}C$ for vegetation samples around the Fontaine Ardente gas seep.

4 Microbial sensors

Development of microbial based sensors has been reported in deliverable 4.3 (2021), however relevant details are summarised below. Additional details for 16S rRNA sequencing using Oxford Nanopore and relative abundance of functional genes are new to this deliverable so additional details are supplied.

4.1 SAMPLE COLLECTION AND METHOD DEVELOPMENT

Water samples were collected from Sleen (2019) and FA Alps site for microbiological analysis. Nanopore sequencing data is presented for the Sleen samples where gas isotope data and sufficient DNA was available, meaning eleven samples from six boreholes were analysed: 6.1, 6.2, 25.1 (single only), 31.2, 32.5 and 69.3. Details for Sleen sample collection and DNA extraction are presented in D4.3 (2021).

4.1.0 Alps Fontaine Ardent field sampling and DNA extraction

To test whether Oxford Nanopore sequencing technology could be successfully deployed in the field, a field laboratory was set up close to Fontaine Ardent field site (Figure 1). This was located at the field accommodation but in a separate building.

Water samples were collected from the main gas seep (FA49), as well as upstream and downstream from this seep. As a comparison the creek was also sampled in two places: in line with the gas seep and approx. 50 m upstream. Containers were rinsed three times in sample water before collection. In the field laboratory 600 to 1000 mL of water sample was filtered through sterile 0.22 µm filter membranes using a hand vacuum pump. DNA was extracted from filter membranes in the field laboratory using a PowerSoil DNA extraction kit (Qiagen, Hilden, Germany) and a DNA extraction blank was conducted at the same time using a swab of the table, after sterilisation, used in the field laboratory. The bead beating step was conducted using an oscillation tool at maximum power for 5 minutes, otherwise manufacturers protocol was followed.

4.1.1 Oxford Nanopore sequencing

Polymerase Chain Reaction (PCR) and DNA sequencing were initially conducted in the field laboratory. Details are the same as the laboratory procedure outlined below except a portable PCR instrument was used (Min16, MiniPCR, Cambridge, MA USA), and the PCR step was performed on pooled duplicates rather than triplicates. The field PCR step was successful for all samples however no successful sequencing reads were obtained due to quality control issue on the sequencing flow cell. The DNA extracts were frozen in the field, shipped on ice and stored at -20C prior to sequencing.

In the BGS laboratory, 16S Barcoding Kit (SQK-RAB204, Oxford Nanopore Technologies, Oxford, UK) was used for sequence analysis for Sleen and FA samples. Primers are supplied in the kit and contain barcodes, adapters and the forward primer 27F (5' - AGAGTTTGATCMTGGCTCAG - 3') or reverse primer 1492R (5' - CGGTTACCTTGTTACGACTT - 3'). The manufactures protocol was followed except that the PCR clean-up step was conducted using ChargeSwitch PCR clean-up kit (ThermoFisher Scientific, Waltham, MA, USA), and PCR step was conducted on duplicate/triplicate 10uL volumes which were the pooled before downstream processing. PCR steps were performed using C1000 Touch thermal cycler (BioRad, Hercules, CA, USA). The DNA library was analysed using Flongle flowcells with R9.4.1 chemistry. After PCR amplification the concentration of DNA of the FA DNA extraction blank was less than detection limit and therefore not sequenced.

Control of the MinION sequencer and DNA basecalling was performed using high accuracy mode on MinIT (Oxford Nanopore Technologies, Oxford, UK). Passed DNA reads (Q score >7) were then analysed using FASTQ 16S pipeline (v2020.04.06) using Epi2Me desktop agent (Oxford Nanopore Technologies, Oxford, UK). The FA samples were all analysed on one flow cell. The Sleen samples were analysed on two separate flow cell runs. First run consisted of eight samples (6.1A, 6.1B, 6.2A, 6.2B, 25.1B, 32.5A, 69.3A and 69.3B) and the second run three samples (31.2A, 31.2B and 32.5B).

Microbial community analysis was performed by selecting the top 12 most common orders, with all other orders grouped and classified and grouped as "other". Prior to Principal Component Analysis (PCA), the number of reads was normalised to total classified reads. Statistical analysis was performed using Past (v 3.16), with PCA in variance-covariance mode. The Sleen data was also analysed using raw species level data as classified by Epi2Me.

4.1.2 qPCR

The abundance of the three genes in groundwater samples were quantified using quantitative real-time PCR in a CFX96 real-time detection system (Bio-Rad Laboratories, Inc., Hercules, CA, USA). The 16S gene was amplified according to Suzuki et al. (2000) by primer pair 1369F (5'-CGGTGAATACGTTCYCGG-3) and 1492R (5'-GGWTACCTTGTTACGACTT-3) and probe (TM1389F 5'-FAM CTTGTACACACCGCCCGTC 3'-TAMRA). A 10-fold dilution series of *E. coli* K12 DNA was used for the standard curve. PCR amplification was performed in 30 µl reactions containing 15 µl Lo-Rox Probe Mix (PCR Biosystems, London, UK), 1.2 µl of both primers (100 pmol/µl), 0.6 µl probe (Eurofins Genomics, Galten, Denmark), 11 µl water and 1 µl TC-DNA. Protocol for qPCR was 3 min at 95°C, followed by 40 cycles of 10 s at 95°C and 30 s at 60°C.

The *pmoA* gene was amplified according to Costello and Lidstrom (1999) with primer pair A189gc (GGNGACTGGGACTTCTGG) and mb661 (CCGGMGCAACGTCYTTACC). For *mcrA* mlas (GGTGGTGTM GGDTTCACMCARTA) and mcrA-rev (CGTTCATBGCGTA GTTVGGRTAGT) were used according to Steinberg and Regan (2008). For both *pmoA* and *mcrA*, the internal standards were based on PCR-derived fragments of target genes cloned into the pGEM-T vector (Promega, Madison, WI, USA) and transformed into *E. coli* JM109. Protocol for qPCR of *pmoA* was 2 min at 95°C, followed by 40 cycles of 10 s at 95°C, 30 s at 64°C, 30 s at 72°C, 6 min elongation at 72°C. Protocol for qPCR of *mcrA* was 2 min at 95°C, followed by 40 cycles of 30 s at 95°C, 30 s at 55.7°C, 30 s at 72°C, 6 min elongation at 72°C. For both genes melt curve analysis was also performed.

4.2 RESULTS AND INTERPRETATION

4.2.1 Nanopore DNA sequencing

The five FA samples had an average of 2948 passed DNA reads (1065 to 4088) giving total yield of 18.5 megabases (Mb) with average Q score 10.74. Passed reads had Q score >7. The first batch of nine Sleen samples had an average of 6473 passed DNA reads (2479 to 14470) giving a total yield of 74.5 Mbases and average Q score of 10.86. The second of three Sleen samples had a total of 50669 passed DNA reads (38028 to 60696) giving yield of 191.4 Mb and average Q score of 11.25. Due to the low number of passed DNA reads (<3000) it is possible that the full diversity of four samples could captured: Flame, Upstream, 6.1A and 32.5A.

The number of classified reads using Oxford Nanopores 16S workflow varied from 31% to 95% of DNA reads per sample (Figure 16), with classification accuracy ranging from 81 to 88% (data not shown). Between the two sites 41 distinct bacterial orders were presented with 27 orders present for FA, 29 orders for Sleen and 15 common to both. 11 orders are only represented by one sample. Burkholderiales dominates all the FA samples, whereas the Sleen samples are dominated by Clostridiales (6.1A and B, 25.1B, 31.2A and 69.3A and B), Nitrospirales (6.2A and B) or Syntrophobacterales (32.5A and B).

PCA was applied to the two sites separately, then combined (Figure 17). No clear grouping can be observed for any of the FA samples when analysed as a single dataset. The Sleen replicates for samples 6.1 and 6.2 cluster close together and in the same quadrant, 6.1A and B are particularity close. These two samples have the most negative $\delta^{13}C\text{-}CH_4$ indicating microbial origin of the methane. 32.5A also clusters with these samples, although this could be due to low number of classified DNA reads. Although the same microbial orders dominate in the replicated samples, in the relative abundance of these and other orders mean the replicates do not always plot close together on the PCA. Overlaying the loading plot indicates that the separation of 31.2B is primarily due to abundance of Clostridiales and separation of 32.5B due to abundance of Syntrophobacterales. When combining the data, the FA samples cluster very closely, along with Sleen 32.5A and 6.2B. 6.1 samples cluster closely together and near. The remaining Sleen samples show large variation.

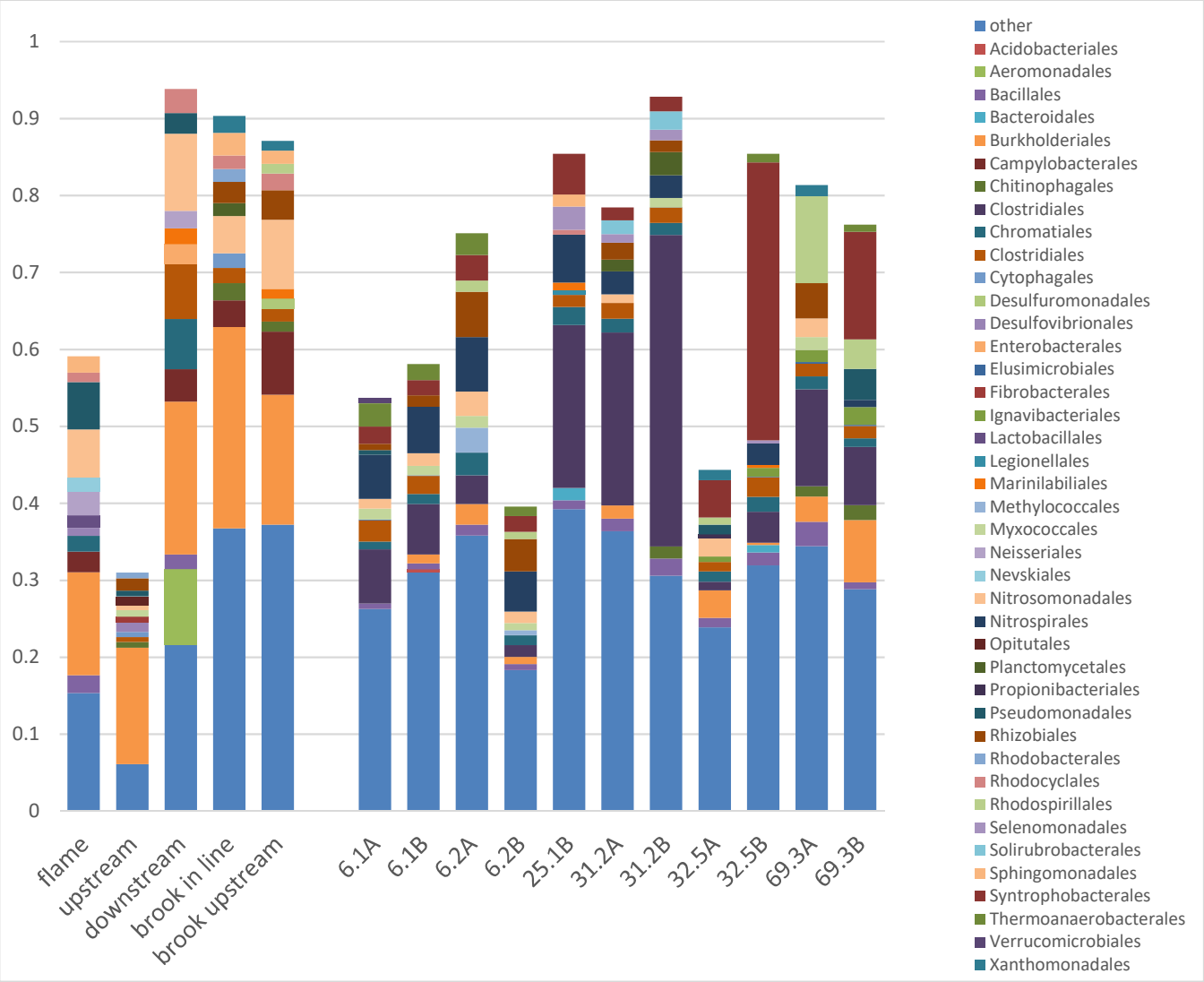

Figure 16. Relative microbial abundances for FA and Sleen water samples. The top 12 Orders for each sample are represented relative to total passed reads for each sample.

Several potential indicator microorganisms were identified in Deliverable 4.3 with *Hyphomicrobium*, *Sphingomonas*, *Xanthobacter*, *Methylomonas* and "*Candidatus* Methanoperedens" as indicators of biogenic methane and *Corynebacterium*, *Nocardia*, *Rhodococcus*, and *Mycobacterium* as indicators of thermogenic methane. "*Candidatus* Methanoperedens" is an archaeon, so will not be detected using the technique used. All except *Mycobacterium* were present in multiple samples (Figure 18). *Hyphomicrobium* and *Sphingomonas* were most commonly found, and dominated the biogenic Sleen samples (6.1 and 6.2). The thermogenic potential indicator microorganisms were only detected a few times, but were more common in thermogenic samples.

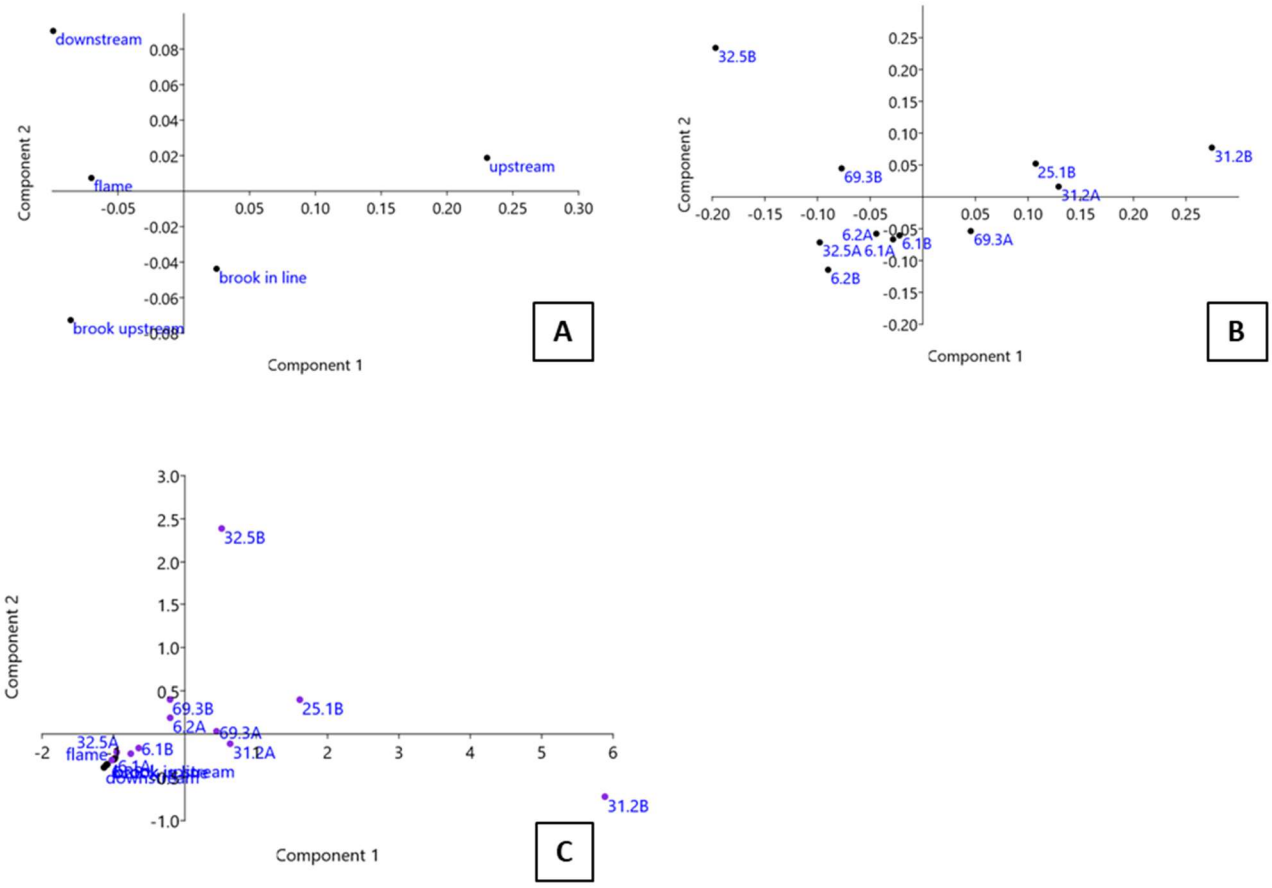

Figure 17. PCA for top 12 microbial orders for each sample. A. FA PC1 70.3%, PC2 14.3%. B. Sleen PC1 51.8%, PC2 29.7%. C. Combined PCA analysis on FA and Sleen microbial order level PC1 82.6% PC2 13.0%

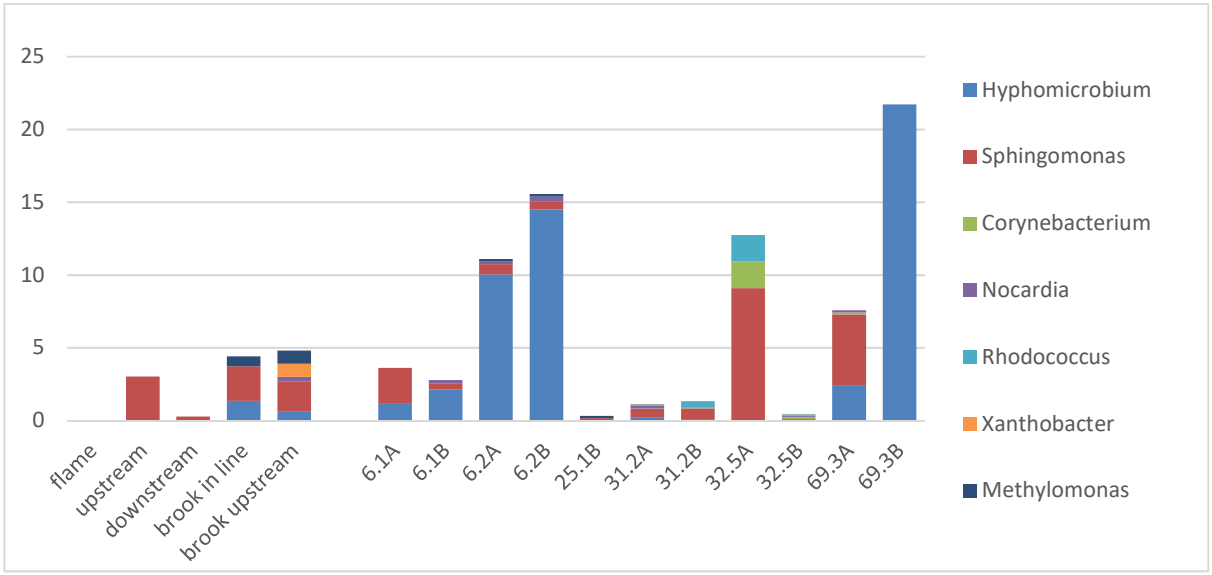

Figure 18. Frequency of potential indicator microorganisms per 1000 reads for each of the samples. No occurrences of *Mycobacterium* were detected in any sample. $\delta^{13}C$ indicative of thermogenic methane FA49 (-27.2‰), Sleen 25.1 (-31.8‰), 31.2 (-29.0‰), 32.5 (-21.65‰) and 69.3 (-21.5‰), $\delta^{13}C$ indicative of biogenic methane Sleen 6.1 (-63.1‰) and 6.2 (-73.6‰).

Nanopore DNA sequencing of the surface water samples from FA and groundwater samples from Sleen resulted in 330 to 47608 classified DNA reads. This large range is due to a combination of factors, including differences in initial DNA extracted from the sample, differences in the number of DNA sequences that can be classified as well as technical difference during data acquisition. Differences in initial DNA input can be overcome in part by adding more DNA, however there was insufficient DNA yield from these samples for this to be possible. Nanopore DNA sequencing analysis workflow applied to these samples uses bacteria 16S rRNA RefSeq database (NCBI BioProject 33175). This database is a curated subset of all DNA sequences deposited in NCBI, therefore it is dominated by health-related samples and environmental samples are underrepresented, especially subsurface environments such as groundwater (Nayfach et al., 2020). This underrepresentation may, in part, contribute towards the difference in the number of unclassified reads (up to 69%). The differences in classified DNA reads is clearly linked to the number of passed reads per sample which varied from 1065 to 60696 depending on the flow cell run. These differences are due to combination of flow cell quality and differences induced during flow cell loading. Flow cells have up to 126 sequencing pores, with minimum threshold of 50, and impurities in samples can affect efficiency of the sequencing pores. As the Flongle flowcells have only been available for general purchase since March 2019, they are continually being developed, these are expected to improvement reliability. If nanopore DNA sequencing is developed into a monitoring technique, minimum sequencing requirements would need to be developed to ensure reliability of data. Although we were not able to complete sequencing in the field this has been demonstrated elsewhere (Parker et al., 2017; Pomerantz et al., 2018), and would mean data could be obtained in near real time.

Applying PCA to the classified DNA sequence data shows no clear separation between the biogenic and thermogenic Sleen samples. However, the biogenic samples cluster closely and the thermogenic samples are widely distributed. This wide distribution could be due to functional genes involved in oxidation of ethane and higher chain alkanes are widely distributed over different microbial groups (van Beilen and Funhoff, 2007), as represented by 16S rRNA. It is surprising that the FA samples cluster closely with the Sleen biogenic samples as their $\delta^{13}C$ indicates a predominantly thermogenic source of the methane and the type of water i.e. stream water vs groundwater, is very different. Further investigations are required to understand these associations.

The similarity between the FA samples and biogenic Sleen samples indicate that multiple factors control the microbial community, but the presence of methane and short chain alkanes may exert a smaller but noticeable effect on these indicator microorganisms. Most of the indicator organisms identified in D4.3 (SECURe report D4.3, 2021)were observed in the samples but in low abundances. Developments in bioinformatics protocols and application of techniques such as 'read until' could be applied to 16s rRNA sequence data to detect specific indicator organisms. This read until function allows for continual sample analysis until a user define threshold is met (Edwards et al., 2020). An alternative use for DNA sequencing technology is to develop methods to analyse appropriate functional genes, for this application those involved in the oxidation of methane (e.g. *pmoA*, *mcrA*) or higher alkanes (e.g. particular variants of soluble di-iron monooxygenases (SDIMO)).

Nanopore sequencing can be successfully applied to groundwater samples with elevated methane. Using the diversity of the 16S rRNA gene tested here does not correlated to methane concentrations or isotopic ratios, indicating multiple influences on the diversity of microbial community. Targeting additional genes such as mcrA or SDIMO is discussed at the end of the subsequent qPCR section.

4.2.2 **qPCR**

A high hydrocarbon concentration is observed in the different wells above the blowout, whereas the concentrations are lower upstream. In Figure 19, these concentrations are plotted against the relative concentration of both *pmoA* and *mcrA*. Both genes are involved in methane oxidation, where *pmoA* is linked to aerobic methane oxidation, and *mcrA* is linked to methanogenesis and anaerobic methane oxidation. There is no clear correlation between hydrocarbon concentrations and the relative abundance of either of the genes. The relative abundance of the *pmoA* gene is only 10^{-3} to 10^{-5} per 16S gene, whereas the relative abundance of *mcrA* gene is higher (10^{-1} to 10^{-3} per 16S gene. The dominance of *mcrA* over *pmoA* is expected in anaerobic wells, such as in the wells with elevated hydrocarbon concentration.

Methane concentration does not seem to be a controlling factor for the relative abundance of either gene (Figure 19). In Figure 20, the relative abundance of both genes are plotted in 3D against CH_4 concentration, $\delta^{13}C$-CH_4 and δD-CH_4 in three different figures. In Figure 20 A and C there appears to be a correlation between *pmoA* and both $\delta^{13}C$-CH_4 and δD-CH_4 when excluding the three higher methane concentrations. In Figure 20 E and F the relative abundance of *pmoA* and *mcrA* are plotted against $\delta^{13}C$-CH_4 and δD-CH_4, respectively. Here, there is seen a correlation with increasing relative abundance of both genes and decreasing isotope ratios (increasing biogenic influence) revealing that the relative abundance of both genes are higher in biogenic

impacted groundwater wells. The trend is most clear for *mcrA*, which is also the gene involved in biological methane production. As illustrated in Figure 9, δ^{13}C-CH_4 higher than -50 are thermogenic and values below -50 are biogenic. For δD-CH_4 values below -150 are biogenic.

As the *mcrA* gene is involved in both biological methane production and anaerobic methane oxidation, the increase in abundance of this gene could be due to an increase in presence of microorganisms capable of either process. However, as a biogenic source of methane is also linked to increasing relative *pmoA* gene concentration (aerobic methanotrophy only), this indicates an increase in methanotrophy potential. Thermogenic sources of methane have higher proportion of ethane and other short chain alkanes (Figure 19). The presence of short chain alkanes increases the diversity of microbial metabolic processes, and microorganisms (van Beilen and Funhoff, 2007), these microorganisms could compete with methanotrophs, therefore reducing their reducing their relative abundance. Two processes, similar to those investigated here, could be used to further understand these differences. The first is to look at quantification of genes involved in oxidation of short chain alkanes by qPCR (e.g. SDIMO). The second technique is to modify the Nanopore DNA sequencing to target the *mcrA* gene, as ANME microorganisms form a distinct group if microorganisms that can be identified by the *mcrA* sequence (Hallam et al., 2003).

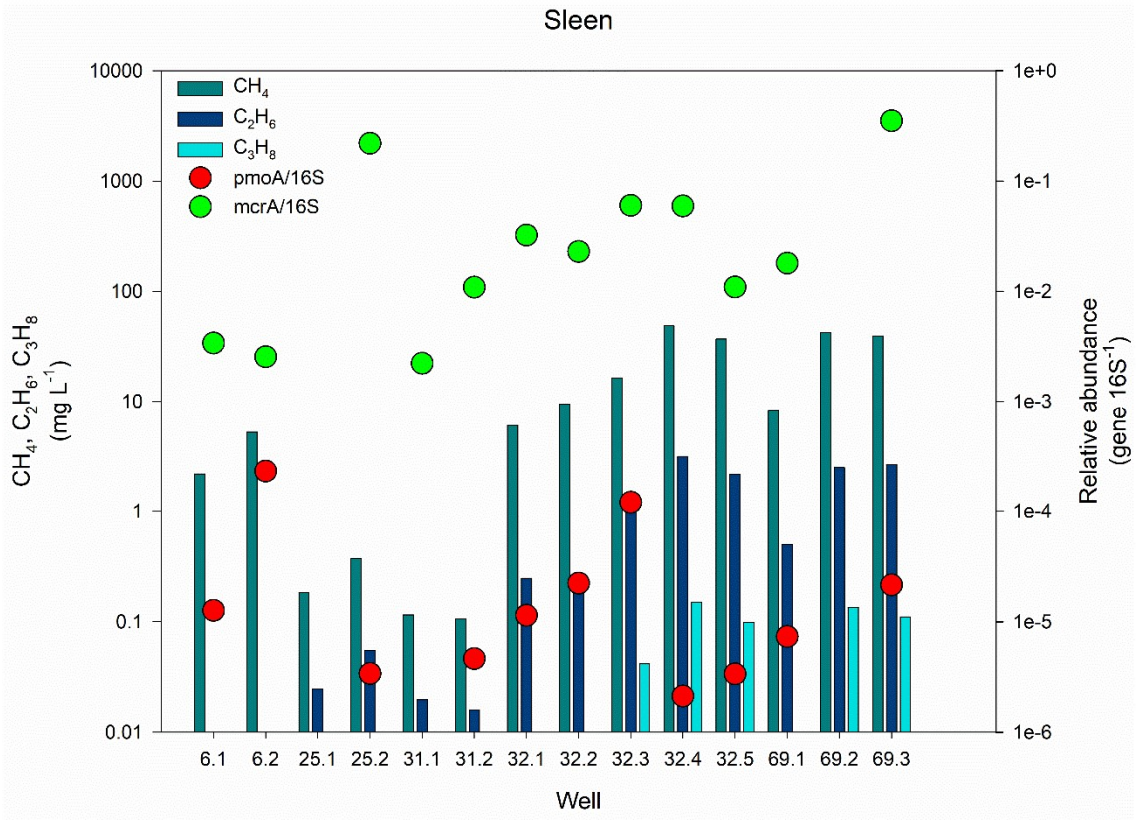

Figure 19. The concentration of CH_4, C_2H_6 and C_3H_8 (mg L^{-1}) and the relative abundance of the *pmoA* and *mcrA* genes in relation to the total bacterial amount (16S). The placement of the different wells is seen in Figure 4.

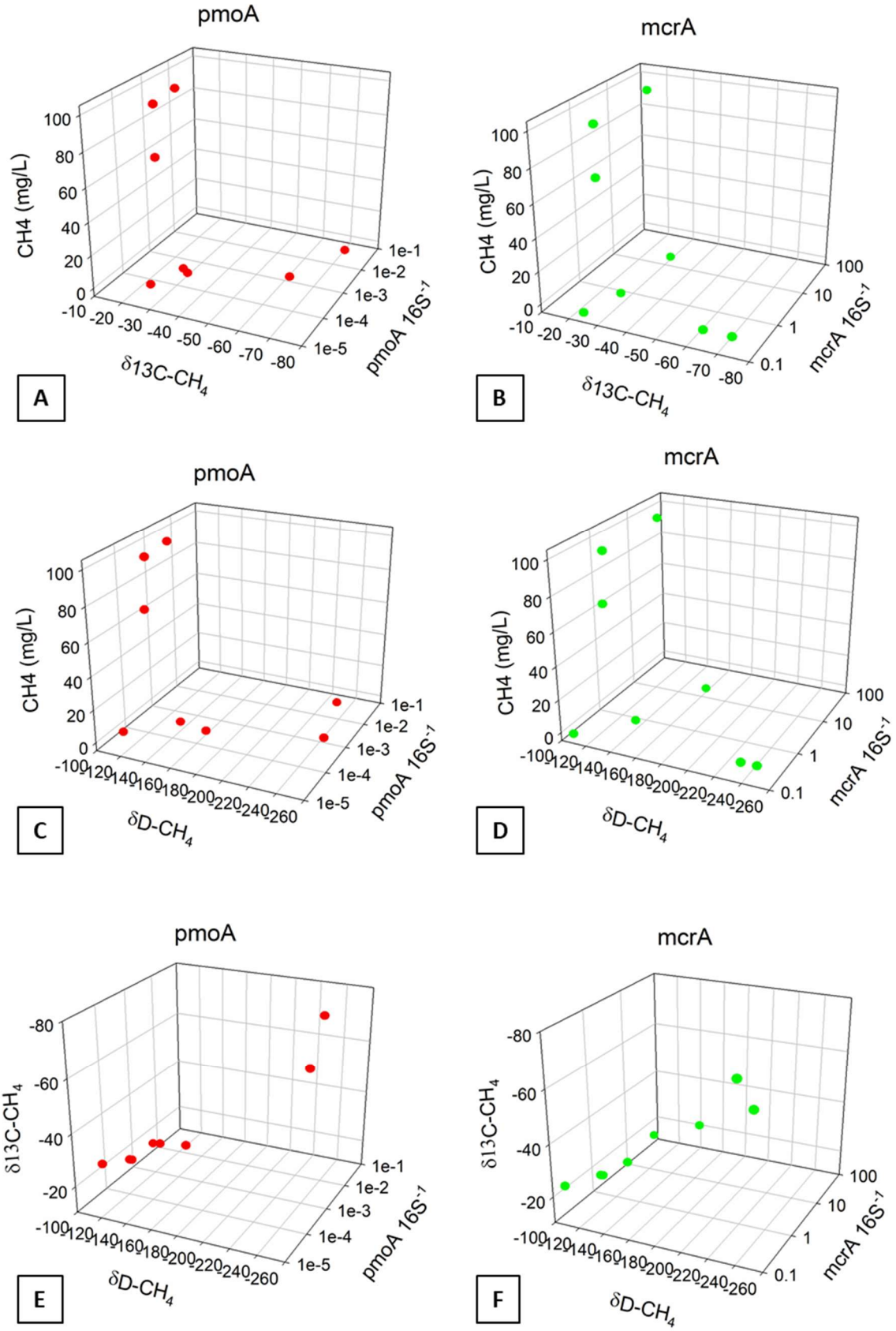

Figure 20. 3D plots for the relative abundance of both *mcrA* and *pmoA* in relation to CH_4 and $\delta^{13}C$-CH_4 (A & B), CH_4 and δD-CH_4 (C & D), and $\delta^{13}C$-CH_4 and δD-CH_4 (E & F).

5 Utilisation of gas and microbial sensors for monitoring gas seepages

The effectiveness of novel isotope-based methodologies and microbial analyses for monitoring gas seepages were studied. Below, the suitability of the tested methods is summarised and recommendations for further research are provided.

5.1 GAS BASED SENSORS

5.1.1 Isotope methods for tracing gas seepage sources

Methane clumped isotope measurements were conducted on gas samples collected from a natural gas seepage (French Alps), a natural gas reservoir (Poland) and a man-induced gas leakage site (Netherlands). Compositional and isotopic analyses suggest that sampled gasses range from thermogenic (deep source rock) to biogenic and possible abiotic gas origin. The current data set adds to an increasing number of methane clumped isotope analyses conducted on a variety of natural settings for deciphering gas' origin. Although the methane clumped isotope technique is rapidly evolving and suggests that promising new insights can be gained by studying the different isotopologues in methane, there are several challenges that make this method not yet mature enough for routine monitoring of gas seepages. The challenges lie in the analytical aspects of the method as well as in the data interpretation.

Analytically, the method is very complex. Sample preparation (gas purification) and data analyses require advanced expertise in sample processing and mass spectrometry techniques. The method is labour intensive with sample gas purification taking about half a day of manual operator input. Mass spectrometer data acquisition takes about 20 hours. While most data acquisition proceeds automatically, expert skills are needed to set up and maintain the machine such that data acquisition is conducted properly. This makes the method currently less suited for rapid and high sample throughput. In addition, only a handful of university laboratories world-wide provide methane clumped analyses on non-commercial, research base (e.g., Stolper et al., 2014a; Wang et al., 2015; Young et al., 2017). IMAU (Utrecht university, The Netherlands) is, to date, the only laboratory that can analyse methane clumped isotopes in gasses that have less than 10% methane concentrations. Such low concentrations are however, often encountered when sampling from soil gas above a (natural) gas leakage site.

The data that is obtained from the methane clumped method may provide promising insights into the origin of gas. However, several processes that may affect the clumping in the isotopologues Δ^{13}CD and ΔDD are not yet fully understood and require further research. Provided that a gas has formed and remained in thermodynamic equilibrium (either for a thermogenic or a biogenic gas), the calculated temperature can be used as a direct proxy for the gas formation temperature. Several of the collected samples in this study (one in Sleen and three in the French Alps[2]) are adhering to this requirement and their calculated temperatures have been used to constrain the source of gas formation. However, there are also samples that are in disequilibrium and the corresponding gas formation temperature cannot be calculated. Processes resulting in Δ^{13}CD and ΔDD disequilibrium may involve mixing of gasses with different origin, isotope fractionation or microbial activity.

Understanding how microbial activity affects methane clumping is not yet fully understood. In the data presented in this report, microbial community diversities and relative abundance of the two genes *pmoA* and *mcrA* has been conducted. Isotopic composition of sampled gases in Sleen or French Alps do not provide single or groups of microbe communities that are indicative for gases from a biogenic or a thermogenic nature. Nonetheless, microbial communities have been shown to affect the clumping (e.g., Stolper et al., 2015; Wang et al., 2015) and therefore require additional research before it can be applied as a monitoring tool for detecting gas leakages.

Despite the research challenges, methane clumped isotope analyses has potential for understanding gas formation processes. Clumped isotope analyses of methane samples from Sleen showed that it may be possible, when the isotope data is combined with for example numerical simulations of basin subsidence and thermal history, to reconstruct the source of the gas in the presence of multiple source rocks. It was also shown

[2] Data awaiting publication and not reported in this report.

that by combining calculated temperatures with modelled burial temperatures for source rocks, it is possible to refine the timing of hydrocarbon charge.

In the case of the methane gas samples analysed from Poland, it was shown that the gas may be composed of a mixture of predominantly thermogenic gas and gas with a abiotic origin. Understanding these components provide insights in mixing processes in the subsurface.

For routine gas seepage monitoring, bulk isotope measurements ($\delta^{13}C$ and δD) are currently better suited for determining the source of gas leakage (biogenic vs thermogenic). Bulk isotopes can also be analysed in rapid succession, high sample throughput and low cost (50-100 euro a sample). Clumped measurements currently are a factor 10-20 more expensive owing to the analytical challenging method and expert skills discussed above. Bulk isotope analyses on gasses in groundwater or seeping through to the surface therefore can be readily used to pin point the source and origin of gas seeps. This applied to both methane and CO_2 bulk isotope analyses.

5.1.2 Carbon-14 as tool for recording long term CO_2 leakage

Carbon-14 analyses on tree rings and leaves around a gas seep at the Fontaine Ardente field site suggest it has the potential to act as an integrator of gas emanation over time. Provided that the tree rings can be dated by dendrology, an archive of gas fluxes may be reconstructed. This offers perspectives of using vegetation carbon isotopes as proxies for present and past gas emanations, including man-induced gas leaks, e.g. from gas storage or natural gas exploitation facilities.

Challenges in this method lie in determining the distances from the CO_2 point source to the trees that incorporate the dead carbon, determining prevailing (historic) wind directions and statistical number of analysed samples. In future research, a more detailed and refined sampling campaign should be considered to account for those variations before the method can be used as a proxy for records of (historic) CO_2 emissions at gas seepage sites.

5.2 MICROBIAL SENSORS

Microbial biosensors are less sensitive to short term fluctuations in gas concentrations, making them a promising option, especially when intermittent leaks are possible.

From the microbial analyses, no clear link between methane (or ethane/propane) concentration and microbial diversity was found. With the preliminary analysis conducted here, the isotopic composition of sampled gasses in Sleen or French Alps do not provide single or groups of microbial communities that are indicative for gases from a biogenic or a thermogenic source. However the thermogenic samples contained more diverse communities and low concentrations of potential indicator microorganisms. The grouping of biogenic samples could be coincidental as there were only two biogenic samples analysed within this report. The link between diversity and indicator microorganisms would need to be explored further by analysing microbial communities from additional samples and detailed bioinformatic exploration of existing data. Further, amplicon sequencing of the two functional genes *pmoA* and *mcrA* could provide additional information on community changes that are not captured in the 16S amplicon approach. Another potential target for this type of amplicon sequencing would be to target the genes responsible for the oxidation of non-methane alkanes, typically members of the soluble di-iron monooxygenase gene family. Additionally, one genus of methylotroph, *Methylocella*, is thought to be associated with natural gas seeps and could be specifically targeted with a qPCR assay (Farhan Ul Haque et al., 2018; Farhan Ul Haque et al., 2019). This work will be conducted in the BGS laboratory on other projects. As we saw an effect of the two genes tested here (Figure 20), we anticipate that an approach using multiple functional genes will provide an indication of the origin of gas seeps.

Field portable DNA extraction and analysis as tested here and demonstrated end to end elsewhere (Parker et al., 2017; Pomerantz et al., 2018) had the potential to provide detailed microbial community analysis within a few hours of sample collection. Although these results are not instant, conducting some or all of the analysis in the field reduces the requirement for large, several litre samples, to be transported, and reduces the risk of the microbial growth during transport. If a local field laboratory is available results can be seen within a field campaign, and additional samples can be collected or sampling strategy altered during a single trip. This could be particularly important if investigating other anomalous results. The wealth of data and flexibility of Nanopore DNA sequencing provides a highly adaptable platform for DNA sequencing. development of this technology, both in bioinformatic analysis to highlight differences in abundance of minor microbiological groups that may

be of interest as well looking into abundance or diversity of functional genes could make this tool a valuable addition to field monitoring campaigns.

The diversity of microorganisms that are culture under a methane and propane headspace was tested as an potential indicator for biogenic and thermogenic methane source. Microbial cell culture is low cost and requires minimal specialist equipment, reagents and expertise. The details of development are contained within D4.3 of the SECURe project (SECURe report D4.3, 2021). The species richness of the microbes grown under methane and propane headspace differed, and could be used to predict the methane ethane ratio of the sample with about 70% accuracy (38 samples from two sites). Further refinements to this procedure, such as identification of outliers and repeat analysis, should improve accuracy, making microbial culture a promising low cost monitoring technique.

5.3 DEVELOPMENTS FOR LONG AND SHORT TERM GAS LEAKAGE MONITORING

Detection subsurface gas leakages (either natural origin or man-induced) necessitates long- and short-term monitoring. In this study, a combination of novel isotope based methodologies and micro-bacterial analyses were used for deciphering the source and origin of gas and reconstruct the long-term baseline record of gas seepage.

These monitoring tools can be applied to monitor gas leakages at different spatial and temporal ranges. Short-term in-situ detection of gas seepages was tested using clumped isotopes to study the origin of methane and/or CO_2 gas by determining its (subsurface) gas formation temperature. The response of microbial communities to those in-situ gas leaks was characterised by identifying specific microbial groups. Methodologies for reconstructing long-term, time averaged records of CO_2 gas seepages were tested by utilising Carbon-14 dating on local vegetation.

The application of methane clumped isotope analyses in various settings (natural gas seepage, natural gas reservoir and a man-induced leakage site) has shown that the technique is suitable for tracing the source and origin of gas. However, for routine gas seeps monitoring, the technique is (analytically) challenging. If the method become less of a research tool but gain more applied traction, then methane clumped isotopes could be a viable addition to the suite of tools for routine gas leakage monitoring. Improvements to raise the TRL for methane clumped isotopes for routine monitoring would require faster data acquisition time, and a reduction of the analytical complexity of measuring clumped isotope compositions. The method would also profit from additional investigations on a variety of natural and induced methane and CO_2 leakage sites.Based on the research presented here, a workflow for in-situ monitoring would involve repeated gas sampling campaigns for bulk isotopic analyses with occasional sampling for clumped isotope analyses when additional insights in the origin of the gas are required.

From the work conducted in Sleen and France, it was concluded that microbial communities have the potential to be used as a monitoring tool. Bacterial activity affects the methane in the subsurface through methanotrophs (organisms able to oxidise methane into CO_2). Two specific types that were studied (pmoA and mcrA; whereby pmoA is linked to aerobic methane oxidation and mcrA to anaerobe methane oxidation and is a marker for biological methane production) showed no clear link between hydrocarbon concentrations and the relative abundance of either genes. It was, however, shown that when the relative abundance of these genes is correlated to the gas isotopic composition, that the relative abundance of both genes is higher in gas that had a biogenic origin compared to a thermogenic origin. It is considered that microbial biosensors are less sensitive to short-term fluctuations compared to gas concentrations. Combined, they may have the potential to act as markers for short term to intermittent gas leakage. The work presented in this report suggests that combining microbial techniques with established geochemical (isotope) methods allows for an accurate assessment of the source of leaking gas.

Glossary

Clumped isotopes Novel isotope technique that uses the bonding (or clumping) of heavy isotopes in a molecule.

FA Fontaine Ardente field site.

ROC Rochasson field site.

$\delta^{13}C$ & δD Bulk carbon ($\delta^{13}C$) and methane (δD) isotope ratio.

$\Delta^{13}CD$ & ΔDD methane clumped isotope ratios used to calculate the methane gas formation temperature.

^{14}C Radiocarbon-14 dating.

Acknowledgements

This work was funded by European Union's Horizon 2020 research grant number No 764531. We would like to thank the Watermaatschappij Drenthe and the landowner for providing access to groundwater monitoring wells at Sleen. Alex Renesse Van Duivenbode is thanked for assistance during the Sleen field sampling campaign and Jasper Griffioen for groundwater discussions. Rader Abdul Fattah and Susanne Nelskamp are thanked for assistance in providing the basin model data from the Sleen region.

We are indebted to Malu Sivan and Elena Popa at the Atmospheric Physics and Chemistry Department of Utrecht University for their perseverance and tenacity in getting the methane clumped isotope method to work in their lab and conducting the analyses on our samples.

References

Cook, A. C., Hainsworth, L. J., Sorey, M. L., Evans, W. C., and Southon, J. R., 2001, Radiocarbon studies of plant leaves and tree rings from Mammoth Mountain, CA: a long-term record of magmatic CO2 release: *Chemical Geology*, v. 177, no. 1, p. 117-131, https://doi.org/10.1016/S0009-2541(00)00386-7.

Costello, A. M., and Lidstrom, M. E., 1999, Molecular characterization of functional and phylogenetic genes from natural populations of methanotrophs in lake sediments: *Applied and Environmental Microbiology*, v. 65, p. 5066-5074, 10.1128/aem.65.11.5066-5074.1999.

Donders, T. H., Decuyper, M., Beaubien, S. E., van Hoof, T. B., Cherubini, P., and Sass-Klaassen, U., 2013, Tree rings as biosensor to detect leakage of subsurface fossil CO2: *International Journal of Greenhouse Gas Control*, v. 19, p. 387-395, https://doi.org/10.1016/j.ijggc.2013.09.017.

Douglas, P. M. J., Stolper, D. A., Eiler, J. M., Sessions, A. L., Lawson, M., Shuai, Y., Bishop, A., Podlaha, O. G., Ferreira, A. A., Santos Neto, E. V., Niemann, M., Steen, A. S., Huang, L., Chimiak, L., Valentine, D. L., Fiebig, J., Luhmann, A. J., Seyfried, W. E., Etiope, G., Schoell, M., Inskeep, W. P., Moran, J. J., and Kitchen, N., 2017, Methane clumped isotopes: Progress and potential for a new isotopic tracer: *Organic Geochemistry*, v. 113, p. 262-282, https://doi.org/10.1016/j.orggeochem.2017.07.016.

Edwards, A., Cameron, K. A., Cook, J. M., Debbonaire, A. R., Furness, E., Hay, M. C., and Rassner, S. M. E., 2020, Microbial genomics amidst the Arctic crisis: *Microb Genom*, v. 6, no. 5, 10.1099/mgen.0.000375.

Eiler, J. M., 2007, “Clumped-isotope” geochemistry—The study of naturally-occurring, multiply-substituted isotopologues: *Earth and Planetary Science Letters*, v. 262, no. 3–4, p. 309-327, http://dx.doi.org/10.1016/j.epsl.2007.08.020.

Eiler, J. M., Bergquist, B., Bourg, I., Cartigny, P., Farquhar, J., Gagnon, A., Guo, W., Halevy, I., Hofmann, A., Larson, T. E., Levin, N., Schauble, E. A., and Stolper, D., 2014, Frontiers of stable isotope geoscience: *Chemical Geology*, v. 372, no. 0, p. 119-143, http://dx.doi.org/10.1016/j.chemgeo.2014.02.006.

Eiler, J. M., Clog, M., Magyar, P., Piasecki, A., Sessions, A., Stolper, D., Deerberg, M., Schlueter, H.-J., and Schwieters, J., 2013, A high-resolution gas-source isotope ratio mass spectrometer: *International Journal of Mass Spectrometry*, v. 335, no. 0, p. 45-56, http://dx.doi.org/10.1016/j.ijms.2012.10.014.

Eldridge, D. L., Korol, R., Lloyd, M. K., Turner, A. C., Webb, M. A., Miller, T. F., and Stolper, D. A., 2019, Comparison of Experimental vs Theoretical Abundances of 13CH3D and 12CH2D2 for Isotopically Equilibrated Systems from 1 to 500 °C: *ACS Earth and Space Chemistry*, v. 3, no. 12, p. 2747-2764, 10.1021/acsearthspacechem.9b00244.

Etiope, G., 2009, Natural emissions of methane from geological seepage in Europe: *Atmospheric Environment*, v. 43, no. 7, p. 1430-1443, https://doi.org/10.1016/j.atmosenv.2008.03.014.

Farhan Ul Haque, M., Crombie, A. T., Ensminger, S. A., Baciu, C., and Murrell, J. C., 2018, Facultative methanotrophs are abundant at terrestrial natural gas seeps: *Microbiome*, v. 6, no. 1, p. 118, 10.1186/s40168-018-0500-x.

Farhan Ul Haque, M., Crombie, A. T., and Murrell, J. C., 2019, Novel facultative Methylocella strains are active methane consumers at terrestrial natural gas seeps: *Microbiome*, v. 7, no. 1, p. 134, 10.1186/s40168-019-0741-3.

Gal, F., Kloppmann, W., Proust, E., Bentivegna, G., Defossez, P., Mayer, B., and Gaucher, E., 2017, Natural CH4 Gas Seeps in the French Alps: Characteristics, Typology and Contribution to CH4 Natural Emissions to the Atmosphere: *Energy Procedia*, v. 114, p. 3020-3032, https://doi.org/10.1016/j.egypro.2017.03.1430.

Gal, F., Proust, E., and Kloppmann, W., 2019, Towards a Better Knowledge of Natural Methane Releases in the French Alps: A Field Approach: *Geofluids*, v. 2019, p. 6487162, 10.1155/2019/6487162.

Gerling, P., Geluk, M. C., Kockel, F., Lokhorst, A., Lott, G. K., and Nicholson, R. A., 1999, ’NW European Gas Atlas’ – new implications for the Carboniferous gas plays in the western part of the Southern Permian Basin: *Geological Society, London, Petroleum Geology Conference series*, v. 5, no. 1, p. 799, 10.1144/0050799.

Gerling, P., Idiz, E., Everlien, G., and Sohns, E., 1997, New Aspects on the Origin of Nitrogen in Natural Gases in Northern Germany: *Geologisches Jahrbuch*, v. Geologisches Jahrbuch, p. 65-84.

Hallam, S. J., Girguis, P. R., Preston, C. M., Richardson, P. M., and DeLong, E. F., 2003, Identification of methyl coenzyme M reductase A (*mcrA*) genes associated with methane-oxidizing archaea: *Appl Environ Microbiol.* , v. 69, no. 9, p. 5483-5491, doi:10.1128/aem.69.9.5483-5491.2003.

Hoefs, J., 2009, Stable Isotope Geochemistry, Springer-Verlag Berlin Heidelberg.

Karion, A., Sweeney, C., Pétron, G., Frost, G., Michael Hardesty, R., Kofler, J., Miller, B. R., Newberger, T., Wolter, S., Banta, R., Brewer, A., Dlugokencky, E., Lang, P., Montzka, S. A., Schnell, R., Tans, P., Trainer, M., Zamora, R., and Conley, S., 2013, Methane emissions estimate from airborne measurements over a western United States natural gas field: *Geophysical Research Letters*, v. 40, no. 16, p. 4393-4397, 10.1002/grl.50811.

Karnkowski, P. H., 2007, Permian Basin as a main exploration target in Poland: *Przegld Geologiczny*, v. 55, no. 12/1.

Knittel, K., and Boetius, A., 2009, Anaerobic Oxidation of Methane: Progress with an Unknown Process: *Annual Review of Microbiology*, v. 63, p. 311-334, 10.1146/annurev.micro.61.080706.093130.

Kotarba, M. J., and Nagao, K., 2015, Molecular and isotopic compositions and origin of natural gases from Cambrian and Carboniferous-Lower Permian reservoirs of the onshore Polish Baltic region: *International Journal of Earth Sciences*, v. 104, no. 1, p. 241-261, 10.1007/s00531-014-1063-0.

Lardie Gaylord, M. C., Longworth, B. E., Murphy, K., Cobb, C., and McNichol, A. P., 2019, Annual radiocarbon measurements in a century-old European beech tree (Fagus sylvatica) from coastal northeastern North America: *Nuclear Instruments and Methods in Physics Research Section B: Beam Interactions with Materials and Atoms*, v. 456, p. 264-270.

Laughrey, C., and Baldassare, F., 1995, Geochemistry and origin of some natural gases in the Plateau Province, Central Appalachian Basin, Pennsylvania and Ohio: *Aapg Bulletin - AAPG BULL*, v. 79, 10.1306/7834D8D2-1721-11D7-8645000102C1865D.

Levin, I., Kromer, B., Schoch-Fischer, H., Bruns, M., Munnich, M., Berdau, D., Vogel, J. C., and Munnich, K. O., 1994, Delta $^{14}CO_2$ records from two sites in Central Europe, *in* Boden, T. A., Kaiser, D. P., Sepanski, R. J., Stoss, F. W., and Logsdon, G. M., eds., *Trends 93: A compendium of data on global change*: Oak Ridge, USA, Carbon Dioxide Information Analysis Centre, Oak Ridge National Laboratory, p. 203-211.

Lubaś, J., Szott, W., Łętkowski, P., Gołąbek, A., Miłek, K., Warnecki, M., Wojnicki, M., Kuśnierczyk, J., and Szuflita, S., 2020, Long-term sequestration process in the Borzęcin structure – observation evidence of the injected acid gas migration and possible leakage, Prace Naukowe Instytutu Nafty i Gazu – Państwowego Instytutu Badawczego.

Luton, P. E., Wayne, J. M., Sharp, R. J., and Riley, P. W., 2002, The mcrA gene as an alternative to 16S rRNA in the phylogenetic analysis of methanogen populations in landfill b: *Microbiology*, v. 148, p. 3521-3530, 10.1099/00221287-148-11-3521.

Nayfach, S., Roux, S., Seshadri, R., Udwary, D., Varghese, N., Schulz, F., Wu, D., Paez-Espino, D., Chen, I. M., Huntemann, M., Palaniappan, K., Ladau, J., Mukherjee, S., Reddy, T. B. K., Nielsen, T., Kirton, E., Faria, J. P., Edirisinghe, J. N., Henry, C. S., Jungbluth, S. P., Chivian, D., Dehal, P., Wood-Charlson, E. M., Arkin, A. P., Tringe, S. G., Visel, A., Consortium, I. M. D., Woyke, T., Mouncey, N. J., Ivanova, N. N., Kyrpides, N. C., and Eloe-Fadrosh, E. A., 2020, A genomic catalog of Earth's microbiomes: *Nat Biotechnol*, 10.1038/s41587-020-0718-6.

Nelskamp, S., 2011, Structural evolution, temperature and maturity of sedimentary rocks in the Netherlands: results of combined structural and thermal 2D modeling [PhD Thesis]: Rheinisch-Westfalische Technische Hochschule, Aachen, Germany, 193 p.

NITG-TNO, 2000, Geological Atlas of the Subsurface of the Netherlands, Explanation to Map Sheet VI: Veendam-Hoogeveen: Utrecht, NITG-TNO, p. 154.

Parker, J., Helmstetter, A. J., Devey, D., Wilkinson, T., and Papadopulos, A. S. T., 2017, Field-based species identification of closely-related plants using real-time nanopore sequencing: *Sci Rep*, v. 7, no. 1, p. 8345, 10.1038/s41598-017-08461-5.

Pomerantz, A., Penafiel, N., Arteaga, A., Bustamante, L., Pichardo, F., Coloma, L. A., Barrio-Amoros, C. L., Salazar-Valenzuela, D., and Prost, S., 2018, Real-time DNA barcoding in a rainforest using nanopore sequencing: opportunities for rapid biodiversity assessments and local capacity building: *Gigascience*, v. 7, no. 4, 10.1093/gigascience/giy033.

Rasheed, M. A., Patil, D. J., and Dayal, A. M., 2013, Microbial Techniques for Hydrocarbon Exploration, *Hydrocarbon*.

Reichel, T., 2013, Groundwater Degassing and Separation of Argon from Air for ^{39}Ar Dating with ATTA [PhD Thesis]: University of Heidelberg, Germany, 142 p.

Schoell, M., 1980, The hydrogen and carbon isotopic composition of methane from natural gases of various origins: *Geochimica et Cosmochimica Acta*, v. 44, no. 5, p. 649-661, https://doi.org/10.1016/0016-7037(80)90155-6.

Schout, G., Hartog, N., Hassanizadeh, S. M., and Griffioen, J., 2018, Impact of an historic underground gas well blowout on the current methane chemistry in a shallow groundwater system: *Proceedings of the National Academy of Sciences*, v. 115, no. 2, p. 296, 10.1073/pnas.1711472115.

SECURe Report D3.4, 2021, Report on downhole monitoring as part of environmental baseline assessment for carbon storage and shale gas development: in preparation.

SECURe report D4.3, 2021, Report on the potential for exploiting methane oxidiser genes for monitoring stray methane intruding into aquifers and assessment of the area that can be monitored, https://www.securegeoenergy.eu/sites/default/files/SECURe_D4.3_Final.pdf.

Steinberg, L. M., and Regan, J. M., 2008, Phylogenetic comparison of the methanogenic communities from an acidic, oligotrophic fen and an anaerobic digester treating municipal wastewater sludge: *Applied and Environmental Microbiology*, v. 74, p. 6663-6671, 10.1128/AEM.00553-08.

Stolper, D. A., Lawson, M., Davis, C. L., Ferreira, A. A., Neto, E. V. S., Ellis, G. S., Lewan, M. D., Martini, A. M., Tang, Y., Schoell, M., Sessions, A. L., and Eiler, J. M., 2014a, Formation temperatures of thermogenic and biogenic methane: *Science*, v. 344, no. 6191, p. 1500, 10.1126/science.1254509.

Stolper, D. A., Lawson, M., Formolo, M. J., Davis, C. L., Douglas, P. M. J., and Eiler, J. M., 2018, The utility of methane clumped isotopes to constrain the origins of methane in natural gas accumulations: *Geological Society, London, Special Publications*, v. 468, no. 1, p. 23, 10.1144/SP468.3.

Stolper, D. A., Martini, A. M., Clog, M., Douglas, P. M., Shusta, S. S., Valentine, D. L., Sessions, A. L., and Eiler, J. M., 2015, Distinguishing and understanding thermogenic and biogenic sources of methane using multiply substituted isotopologues: *Geochimica et Cosmochimica Acta*, v. 161, p. 219-247, https://doi.org/10.1016/j.gca.2015.04.015.

Stolper, D. A., Sessions, A. L., Ferreira, A. A., Santos Neto, E. V., Schimmelmann, A., Shusta, S. S., Valentine, D. L., and Eiler, J. M., 2014b, Combined 13C–D and D–D clumping in methane: Methods and preliminary results: *Geochimica et Cosmochimica Acta*, v. 126, p. 169-191, https://doi.org/10.1016/j.gca.2013.10.045.

Stopa, J., Kosowski, P., Wojnarowski, P., and Dziadkiewicz, M., 2017, Experience and prospects of acid gas sequestration in Poland, International Gas Union Conference Rio: Rio de Janeiro, Brazil, p. IBP0751_0717.

Stopa, J., Lubas, J., and Rychlicki, S., 2006, Underground storage of acid gas in Poland - experiences and forecasts, 23rd World Gas Conference: Amsterdam, The Netherlands.

Suzuki, M. T., Taylor, L. T., and DeLong, E. F., 2000, Quantitative analysis of small-subunit rRNA genes in mixed microbial populations via 5'-nuclease assays.: *Applied and environmental microbiology*, v. 66, p. 4605-4614, 10.1128/AEM.66.11.4605-4614.2000.

ten Veen, J. H., Geel, C. R., Kunakbayeva, G., Donders, T. H., and Verreusel, R. M. C. H., 2011, Property prediction of Plio-Pleistocene sediments in the A15 shallow gas systems: TNO, TNO-060-UT-2011-01184/C, 113 p.

TNO-GSN, 2021, Limburg Group, *Stratigraphic Nomenclature of the Netherlands, TNO – Geological Survey of the Netherlands*: Accessed on 28-02-2021 from http://www.dinoloket.nl/en/stratigraphic-nomenclature/limburg-group.

van Beilen, J. B., and Funhoff, E. G., 2007, Alkane hydroxylases involved in microbial alkane degradation: *Appl Microbiol Biotechnol*, v. 74, no. 1, p. 13-21, 10.1007/s00253-006-0748-0.

Wagner, M., Wagner, M., Piske, J., and Smit, R., 2002, Case Histories of Microbial Prospection for Oil and Gas, Onshore and Offshore in Northwest Europe, *in* Schumacher, D., and LeSchack, L. A., eds., *Surface Exploration Case Histories: Applications of Geoschemistry, Magnetics, and Remote Sensing*, American Association of Petroleum Geologists.

Wang, D. T., Gruen, D. S., Lollar, B. S., Hinrichs, K.-U., Stewart, L. C., Holden, J. F., Hristov, A. N., Pohlman, J. W., Morrill, P. L., Könneke, M., Delwiche, K. B., Reeves, E. P., Sutcliffe, C. N., Ritter, D. J., Seewald, J. S., McIntosh, J. C., Hemond, H. F., Kubo, M. D., Cardace, D., Hoehler, T. M., and Ono, S., 2015, Nonequilibrium clumped isotope signals in microbial methane: *Science*, v. 348, no. 6233, p. 428, 10.1126/science.aaa4326.

Whiticar, M. J., 1999, Carbon and hydrogen isotope systematics of bacterial formation and oxidation of methane: *Chemical Geology*, v. 161, no. 1, p. 291-314, https://doi.org/10.1016/S0009-2541(99)00092-3.

Young, E. D., Kohl, I. E., Lollar, B. S., Etiope, G., Rumble, D., Li, S., Haghnegahdar, M. A., Schauble, E. A., McCain, K. A., Foustoukos, D. I., Sutclife, C., Warr, O., Ballentine, C. J., Onstott, T. C., Hosgormez, H., Neubeck, A., Marques, J. M., Pérez-Rodríguez, I., Rowe, A. R., LaRowe, D. E., Magnabosco, C., Yeung, L. Y., Ash, J. L., and Bryndzia, L. T., 2017, The relative abundances of resolved $^{12}CH_2D_2$ and $^{13}CH_3D$ and mechanisms controlling isotopic bond ordering in abiotic and biotic methane gases: *Geochimica et Cosmochimica Acta*, v. 203, p. 235-264, https://doi.org/10.1016/j.gca.2016.12.041.

Young, E. D., Rumble, D., Freedman, P., and Mills, M., 2016, A large-radius high-mass-resolution multiple-collector isotope ratio mass spectrometer for analysis of rare isotopologues of O2, N2, CH4 and other gases: *International Journal of Mass Spectrometry*, v. 401, p. 1-10, https://doi.org/10.1016/j.ijms.2016.01.006.

